Water Supply



Water Supply Vol 22 No 9, 7197 doi: 10.2166/ws.2022.274

# Implications of evolution of circulation patterns on nutrients regime from 2008–2018, in Xiangxi Bay of the Three Gorges Reservoir, China

Umar Ijaz[a,*], Xingxing Zhao[a], Huma Ayub[b], Zaiqiang Cheng[a], Siqian Qiu[a] and Abrar Niaz[c]

[a] College of Hydraulic and Environmental Engineering, China Three Gorges University, 8 Avenue, daxue road, Xiling distric, Yichang 443002, Hubei, China
[b] Department of Zoology, MUST University, Mirpur, AJK, Pakistan
[c] University of Azad Jammu and Kashmir, Muzaffarabad, Pakistan
*Corresponding author. E-mail: umarijaz460@yahoo.com

## ABSTRACT

A 2-D CE-QUAL-W2 hydrodynamic and water quality model was established from 2008 to 2018 in Xiangxi Bay (XXB). The recently built upstream Xiluodu, Wudongde, Xiangjiaba and Beihtan dams have altered the ecohydrology of mainstream and tributaries, so nutrients regime during pre and post dam stages are comparatively investigated here. Although total phosphorus (TP) increased at the lower reach, eutrophication remained TP limited with few exceptions. Maximum supply from main stream, potential of water exchange on surface corresponding to increased overflow intrusion facilitated increased average total nitrogen (TN) at euphotic zone in XXB by 0.1, 0.3 and 0.6 mg/L respectively since 2014. Eutrophication and algal growth in XXB remained TP limited with few exceptions at the upper reach. Average TN increased by 0.1, 0.3 and 0.5 mg/L at the upper, middle and lower reaches respectively in Late March since 2014 compared to those in early years. It increased by 0.2, 0.4 and 0.6 mg/L at the upper, middle and lower reaches in Early April since 2014. It increased by 0.3, 0.6, and 0.9 mg/L at the upper, middle and lower reaches in mid April since 2014. It increased slightly at the upper reach, 0.6 mg/L at the middle reach and 0.9 mg/L at the lower reach during late April. It increased slightly at the upper reach and by 0.3 mg/L at the middle reach and by 0.5 mg/L at the lower reaches corresponding to either of the patterns. During mid May, it remained the same at the upper reach, decreased by 0.2 mg/L at the middle reach and 0.5 mg/L at the lower reach. During late May, it remained the same at the upper reach, decreased by 0.4 mg/L at the middle reach and 0.6 mg/L at the lower reaches. These statistics indicate average an increase in TN in spring except in late May .TN concentration was beyond danger limit sustaining and prolonging eutrophication status in spring. As overflow, interflow and upper interflow patterns are prevalent in random order so nutrients could not be predicted theoretically, however nutrients management from non-point sources and the main supplier Three Gorges Reservoir is advisable.

**Key words:** CE-QUAL-W2, density currents, eutrophication level, nutrient distribution, Three Gorges Reservoir

## HIGHLIGHTS

- Continuous and increased overflow intrusion from the Three Gorges Reservoir (TGR) caused increase in total nitrogen (TN) concentration at upper, middle and lower reaches since 2014.
- TN and total phosphorus (TP) concentration were beyond pollution indices.
- TN/TP ratio declares eutrophication in XXB as TP limited in spring.
- All non-points sources inputs containing TN should be controlled to inhibit algal growth.
- As overflow is prevalent in random order so nutrients are not predictable.

## GRAPHICAL ABSTRACT

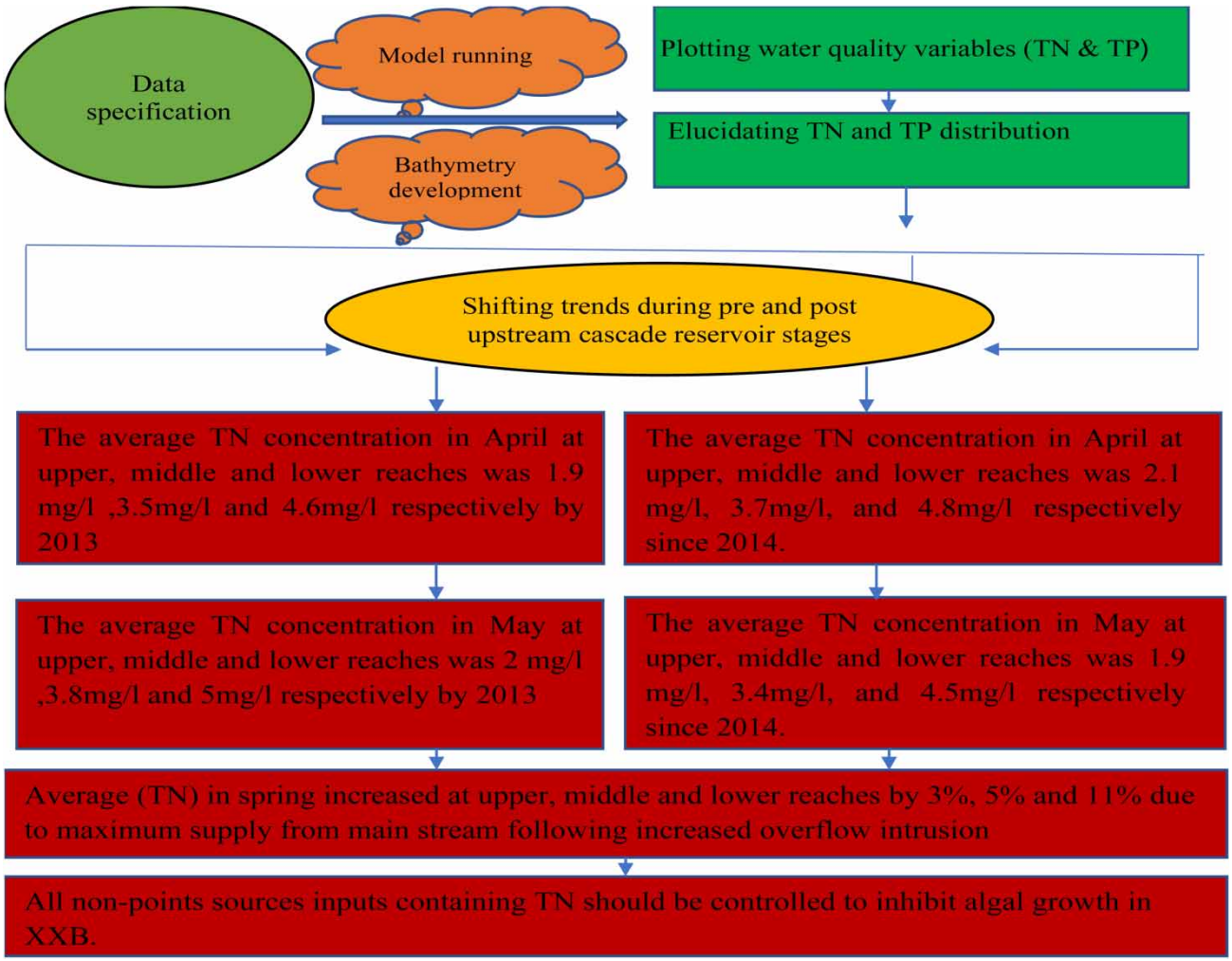


## 1. INTRODUCTION

Water quality and nutrients distribution in lakes and reservoirs depend on density driven water circulation patterns besides meteorological conditions (Yang *et al.* 2017; Wang *et al.* 2018). Nutrient distribution is also dependent on heterogeneity of external sources and anthropogenic activities. (Ambrose *et al.* 2009; Yuan *et al.* 2014). Anthropogenic impacts such as intensive agriculture, eutrophication, livestock growth, dam structures, and global warming added to the nutrients content and vulnerability of lakes (Wu *et al.* 2017; Wang *et al.* 2018) and were deemed as a major threat to the eco-environment of aquatic systems. Water quality parameters including nutrients in aquatic ecosystem are controlled by either point or non-point sources pollution and density current patterns (Chuo *et al.* 2019). Nutrients and dissolved oxygen give shape to the eco-environment of water bodies (Andersen *et al.* 2020; Nwankwegu *et al.* 2020). More water age and temperature stratification favors eutrophication at the surface layer and anoxic conditions in deep water of reservoirs (Sun *et al.* 2021; Xu *et al.* 2021). Nutrients are usually blended with the upper layer of water body owing to mixing, where these could twirl algal growth (Lai *et al.* 2014; Yang *et al.* 2017).

Nutrients favoring algal blooms were concentrated in most of the tributary bays of the Three Gorges Reservoir (TGR) since it started operating (Bartosiewicz *et al.* 2016; Wu *et al.* 2017). Lesser mixing, slow water speed in Xiangxi Bay (XXB) XXB favor nutrients accumulation at the surface, especially in spring (Gao *et al.* 2018; Li *et al.* 2020b). The bidirectional density currents affect ecohydrology and water quality indices of a tributary (XXB) (Andersen *et al.* 2020; Nwankwegu *et al.* 2020). Water circulation patterns following overflow, underflow and lower interflow intrusions are favorable in nutrients rise and are

considered as favorable patterns, while upper interflow and interflow intrusions are ineffective in tackling nutrients rise and are termed as unfavorable patterns (Yang *et al.* 2018b; Zhao *et al.* 2021).

Spatiotemporal distribution of nutrients in bays rely on back and forth flow between bays and reservoirs (Chuo *et al.* 2019; Li *et al.* 2020b). Hydrodynamic and water quality simulation models are useful to analyze density driven currents and implications on nutrients distribution (Wu *et al.* 2017; Li *et al.* 2020b). Critical depth theory also verified a reduced distribution of nutrients at the surface following overflows and underflows and a high concentration of nutrients following upper interflow and interflow intrusions (Liu *et al.* 2012; Bartosiewicz *et al.* 2016).

Hydrodynamics controlling nutrients distribution and algal regime depend on the ratio of favorable and unfavorable circulation patterns (Ji *et al.* 2017). As overflow intrusion was increased during the post upstream cascade reservoirs stage by 30% per annum (Ijaz *et al.* 2022), so nutrients are supposedly well-mixed and less accumulated on the surface.

Differences in surface area, solid substances, density and flow regime cause eutrophication and water quality differences among bays and main reservoirs (Ji *et al.* 2017). The effects of post upstream cascade reservoirs altered density current patterns (Ijaz *et al.* 2022) on eutrophication level and nutrients distribution are vital to justify the viability of eco-environmental friendly operation (EEFO).

Mainstream water provides sufficient nutrients to the epilimnion in XXB during spring and summer, which favors algal growth and eutrophication (Wu *et al.* 2017; Yang *et al.* 2018b). Altered flow dynamics in lakes and reservoirs could affect nutrients distribution and blending through an altered mixing regime (Liu *et al.* 2012). Post TGR hydrodynamic changes posed substantial effects on water quality, nutrients distribution and algal regime in bays (Chuo *et al.* 2019; Li *et al.* 2020b).

Epilimnetic bubble-plume mixing (EM) also verified increased mixing corresponding to increased inflow (Chen *et al.* 2018). Increased nutrient loads and changed nutrient ratios in estuarine waters enhance the occurrence of eutrophication and harmful algae (Bartosiewicz *et al.* 2016). Sufficient nutrients distribution at the surface layer within euphotic depth give rise to algal growth and eutrophication in reservoirs and tributaries (Yu & Wang 2011). Integrated strategies of hydrological management, nutrient concentration control, biological predation and selective reservoir operation could help in controlling eutrophication and algal growth (El-Serehy *et al.* 2018). Nutrients distribution exceeding danger limits and eutrophication cause threats to the aquatic ecosystem through deteriorating water quality, triggering changes in food webs (Spears *et al.* 2013; Passy *et al.* 2016). Therefore, research on the effects of shifts in density flow regime on nutrients distribution is significant to exquisitely determine countermeasures. El-Serehy *et al.* (2018) disclosed through experiments that total nitrogen (N) and dissolved silicate ($Si0_2$) play a more significant part in the freshwater ecosystem than phosphorus. Algal blooms are the result of specific concentrations of hydrological and nutrient parameters and so identifying these thresholds could expedite management of the reservoir through algal mass check (Ai *et al.* 2015).

Nutrient loading from non-point sources associated with anthropogenic activities is one of the major threats for the eco-environment in reservoirs for fostering algal growth (Smith 1982). Increased algal abundance on account of increased nutrients reduces dissolved oxygen concentrations and brings changes to algal assemblage composition (Yuan *et al.* 2014). Nutrients, especially TN, are the best determinant for algal blooms in XXB during spring, so controlling TN and TP could inhibit algal growth (Yuan *et al.* 2014). Alarming thresholds for TN and TP are developed to be controlled to expedite the management of lakes and reservoirs (Bernhardt 2013; Finlay *et al.* 2013). All known techniques for controlling nutrient loading could be tested to avoid TN and TP alarming limits (Yuan *et al.* 2014).

Agricultural activities and farming are major causes of TN rise in lakes and reservoirs (Bernhardt 2013). Based on sensitivity analyses of major descriptors to algal dynamics, TN was found as an important indicator for algal growth (Kim *et al.* 2019). Artificial neural network (ANN) modelling reflected that short-term variations in water quality variables, especially nutrients, continuously shape algal dynamics. Quantile regression analysis have proved TN concentrations of 1 mg/L at the surface as threatening to water quality (Mamun & An 2017).

Similar assosiations of TN with algal blooms were evaluated in an investigation of 30 lakes in China (Wu *et al.* 2017). As limited discharge is not always viable owing to water requirement, so weirs and pulse flow discharges could be adopted to control nutrient loading (Kim *et al.* 2019). Elevated concentration of fertilizers used in the fields is the significant source of nutrients [nitrogen (N) and phosphorus (P)] in main streams and reservoirs (Mamun & An 2017). The extortionate level of nutrients (N and P) fosters eutrophication and quality deterioration in the reservoirs. N-limitation of algal blooms took place in the reservoirs at low-latitude region owing to the geological phenomenon of a tectonic plate (Zhou *et al.* 2017).

In China reservoirs built in the monsoon-region get the maximum monthly inputs of P and N during the summer monsoon period (Passy *et al.* 2016). Empirical modelling evaluated that algal mass had a positive linear dependence (Yuan *et al.* 2014)

on the concentrations of TN and TP in XXB. Overall, research on 182 reservoirs implied that phosphorus was the key nutrient controlling the algal growth. As the TGR and XXB are at low latitudes, so algal blooms can be declared as nitrogen limited (El-Serehy *et al.* 2018). The empirical models for lakes in North America, Europe and Asia (Japan) suggested that the reservoirs are P-limited and the N contributed minorly in algal growth (Passy *et al.* 2016; Mamun & An 2017). Almost >50% of 182 reservoirs were found eutrophic on account of TN, TP and CHL-a values, so the checks on P, emanated mainly from rigorous cultivation activities (fertilizers of N and P from rice fields and meadows), is due for the productive reservoir administration (Mamun & An 2017).

Although XXB is P-limited for algal growth in autumn, TP and TN enrichment crucially fostered algal growth (Nwankwegu *et al.* 2020). Collective nutrients depletions, especially TP control, are required to inhibit algal bloom risk in the TGR (Huang *et al.* 2020; Nwankwegu *et al.* 2020).

Multiple research projects have elucidated that decreasing nutrients inputs is the most productive way to control algal growth (El-Serehy *et al.* 2018) and continuous nutrient recycling (Sepehri *et al.* 2020). In general, marine ecosystems are referred to as TN limited, whereas freshwater ecosystems are TP limited (Huang *et al.* 2020). Ly *et al.* (2014) validated that nutrient limitations in miscellaneous aquatic ecosystems does not seem to conform to a general rule. Co-limitations by TN and TP have also been illustrated in both freshwater and marine ecosystems (Paerl *et al.* 2016). Nutrient limitation transitions could take place in accordance with these changes. Andersen *et al.* (2020) reported TP spatial limitation in the main-stream and TN spatial limitation in Xiangxi River, China. Algal blooms in lentic ecosystems heavily relies on TP distribution and that annual mean TP could predict the average algal existence (Huang *et al.* 2020). Conversely, empirical models of log-transformed Alg-TN and TN:TP-TN expressed less reliance. Algal blooms in spring are TN limited in XXB. As per alterations in TSI (Alg) with TSI (TP) and TSI (SD) agricultural reservoirs were found TP limited ($R^2 = 0.69$), whereas the eutrophication of estuarine and power generation reservoirs and natural lakes was found dependent on non-algal turbidity (Mamun & An 2017; El-Serehy *et al.* 2018).

A reservoir's trophic level (hypereutrophic, eutrophic, mesotrophic, or oligotrophic) can be determined using a combination of water quality parameters such as total phosphorus (TP), total nitrogen (TN) and algal concentration (Mamun & An 2017).

If CHL-a: TP is low then algal chlorophyll will be limited by other parameters (TN, water temperature, light, or precipitation) instead of TP. Conversely, if the CHL-a: TN ratio is high then algal chlorophyll will be TN limited (Spears *et al.* 2013; Paerl *et al.* 2016). Aquatic ecosystems are deemed as N limited if the TN:TP becomes less than 10 and P limited if the ratio becomes greater than 20; co-limitation is believed when the ratio lies in between 10 and 20 (Huang *et al.* 2020).

Correlation analysis and linear regression method indicated a definite role of ecological parameters (including total nitrogen, total phosphorus, water temperature, transparency and dissolved oxygen) on the algal regime in aquatic environments (Yuan *et al.* 2014). Water quality status is multivariate and relies on concentration, deviation and degradation of phosphorus and nitrogen. In order to maintain water quality, TN and TP are required to be within optimal ranges, otherwise they become detrimentally noxious (Atique & An 2019).

The water body is declared highly enriched if TN exceeds 1000 μg/L. As per the unanimously agreed range, a mean Chl-a of 150 mg/m$^2$ reflects nuisance levels (Atique & An 2019). Water resources in most of the regions are threatened to eutrophication, and sustainable management is always due. Water quality, degree of eutrophication and vulnerability to algal growth depend upon cumbersome interactions among nutrient resources, hydrodynamics and ecosystem processes (Bartosiewicz *et al.* 2019).

Nutrient cycling and food web interactions play a significant role in the primary productivity of algal blooms (Paerl *et al.* 2016). Nutrients and light are deemed as the most commonly found environmental factors controlling eutrophication and bio productivity in lakes and reservoirs (Chen *et al.* 2018).

It is well known that changes in nutrient concentration and stoichiometry, such as decreasing of total nitrogen (TN), favors phytoplankton shifting to algal blooms (Paerl *et al.* 2016; Bartosiewicz *et al.* 2019). Additive impacts of stratification and variable nutrient ratios lead to the proliferation of algal blooms in stratified waterbodies, especially in lakes (Bartosiewicz *et al.* 2019).

Additive impacts of warming, temperature stratification and nutrient loading can increase the abundance of algal growth at the surface of lakes and bays (Gao *et al.* 2018). Algal biomass is controlled by nutrient and temperature alterations, with the former being three times more effective than the latter (Bartosiewicz *et al.* 2019). Stratification and mixing in aquatic systems depend upon density current patterns (Xu *et al.* 2021), potentially altering the nutrient cycling and algal mass (Bartosiewicz

*et al.* 2016). The nutrients such as TN, TP etc. foster and reflect eutrophication and algal blooms (Stow *et al.* 2015). An approach to investigate yearly and seasonal fluctuations in nutrient concentrations corresponding to water flow reflect bio-productivity in fresh water bodies (Stow *et al.* 2015). Hence, altered water circulation patterns across seasons and years and their implications on nutrients were investigated through modelling.

The nutrient supplies in strong sensitive areas at the terminal of backwater mainly came from the upstream inflow, and the contribution rate reached more than 85% (Huang *et al.* 2020; Nwankwegu *et al.* 2021). In the weak sensitive area of the downstream, the nutrient content was mainly from the main stream reaching more than 80 and 20% from other tributaries basins (Yang *et al.* 2018a; Huang *et al.* 2020).

The TN concentration was higher in the downstream and upstream and was relatively lower in the middle reach of the XXB (Ma *et al.* 2015), but this trend was found changed for the latter period by Yang *et al.* (2018a), who determined a higher concentration of nitrogen at the lower reach and lesser at the upstream of XXB. The TP concentration at the upstream is higher than downstream and altered in concentration across seasons (Yang *et al.* 2018b).

Among different intruding positions, overflow intrusion supplies the maximum part of nutrient to euphotic depth of the XXB. Interflow intrusion supplies the second largest part of nutrient to euphotic depth of the XXB. Underflow intrusion from the bottom layer supplies the smallest part of nutrient to euphotic depth of the XXB (Ma *et al.* 2015; Xia *et al.* 2018).

The TN concentration remains relatively stable, while the TP undergoes considerable seasonal variations ($p < 0.05$). The least TP concentrations observed were $0.16 + 0.11$ and $0.10 + 0.00$ $\mu gL^{-1}$ during autumn and spring, respectively, revealing TP as the limiting factor in XXB.

The maximum concentrations in TP were observed during summer ($0.93 \pm 0.13$ $\mu gL^{-1}$) and winter ($0.70 \pm 0.092$ $\mu gL^{-1}$). The seasonal dynamics in the TN/TP ratio were $20.37 \pm 0.19$ in spring, and $6.44 \pm 1.91$ during summer. This reflects that the dynamics in the TN/TP stoichiometry is mainly governed by seasonal variation in the TP concentrations (Nwankwegu *et al.* 2021).

If TN/TP $< 9$ characterizes N limitation while TN/TP $> 20$ reflects p-limitation, thus TN/TP in a single year revealed strong N limitation in summer and P limitation in spring (Nwankwegu *et al.* 2021).

As the process of denitrification is effective in controlling the excess N-input into freshwaters, so P-alone was desired to be reduced in the past to control algal blooms (Nwankwegu *et al.* 2020). Subsequently, further studies elucidated that different algal blooms react differently to a varying nutrients including N, P (Coronado-franco *et al.* 2018; Wu *et al.* 2017), hence only TP management protocol would no longer work in inhibiting algal bloom.

Yang *et al.* (2018a) observed TN and TP at site XX06 in XXB from January to February, 2010 and elaborated TN irregular fluctuations between 0.50 and 2.50 $mg{\cdot}L^{-1}$; TP increased slightly from 0.80 to 1.30 $mg{\cdot}L^{-1}$. However, in stage II, TN and Si both declined sharply, but TP increased from 0.10 $mg{\cdot}L^{-1}$ to nearly 0.30 $mg{\cdot}L^{-1}$.

This shows intra-seasonal and seasonal irregular dynamics, which points to a dire need for further investigation over longer time series encompassing pre and post cascade reservoir stages.

Vertical nutrient transport affects the thickness of the euphotic layer and nutrients distribution in lakes and reservoirs (Andersen *et al.* 2020). Hydrodynamic, suspended load and nutrient differences cause spatial diversity in water quality (Xiang *et al.* 2021).

Non-point source pollution foster TN and TP values (Xiang *et al.* 2021), nutrient sources in XXB are non-point sources (Gao *et al.* 2018), therefore nutrients fueling algal blooms are viable. Although hydrological variables, pollution, nutrients, and biochemical indices were investigated for the TGR by Xiang *et al.* (2021), the effects of upstream cascade reservoirs on density currents in collaboration with nutrients and eutrophication level are still vague and unexplored. Spatiotemporal difference of nutrients cause spatiotemporal difference of algal blooms. Nutritional water treatment, non-point source pollution control and hydrodynamic parameters (temperature and discharges) controls could be focused more for reservoir management.

TN and TP concentrations in spring were validated in collaboration with effective and ineffective patterns during pre and post cascade reservoirs stages. Based on these variations, eutrophication level, limiting factor and susceptibility of XXB to algal growth and countermeasures could be predicted.

The mean TN concentrations in TGR were almost 1–3 and 0.05–0.61 mg/L respectively in XXB before upstream cascade reservoirs, complying with pollution indices (Gao *et al.* 2018; Xia *et al.* 2018; Li *et al.* 2019). Since upstream newly built Xiluodu Dam (XLD), Wudongde Dam (WDD), Xiangjiaba Dam(XJB) have changed the thermal and discharge dynamics of mainstream TGR, the altered distribution of nutrients requires evaluation.

The CE-QUALITY-MODEL was developed by Ma *et al.* (2015) and (Xu *et al.* 2021) for a certain period prior to upstream dams and for a selective period in 2016 respectively, but 2D and 3D plots confined to randomly selected julian days from across the seasons were investigated. These attempts were useful to give quantitative information about nutrients spatial distribution and eutrophication degree in XXB. The aforementioned scholars did not analyze and discuss variations in spatial trends except at three specific sites, moreover, no responsiveness of nutrients limitation fluctuations corresponding to shifting trends in circulation patterns were adressed. Li *et al.* (2019) also performed experiments on water samples obtained in 2019 to make imperative developments regarding nutrients spatial distribution. However, lack of modelling investigations of hydrodynamics and temporal variations in sample collections caused knowledge dearth regarding effects of shifting trends in density current patterns on nutrints spatial distribution. The evaluation of exact field values of nutrients are also vulnerable to be altered in lab experiments in spite of well-equipped storage. Obtaining of samples for a particular moment of time could also be misleading.

Non of the previous researches have comparatively investigated variations in nutrients spatial distribution, limitation factors and eutrophication degree prior to and post upstream built cascade reservoirs since 2014.

Spatiotemporal transport mechanisms rely on water age, velocity and mixing, which ultimately define nutrients distribution in XXB (Wang *et al.* 2018; Li *et al.* 2020a). In spite of elucidation of altered TGR thermal developments, circulation patterns, water age and mixing by Ijaz *et al.* (2022), quantitative impacts on spatiotemporal distribution of nutrients in XXB during both stages were not correlated through observed and simulated data. The effects of shifts in favorable and unfavorable patterns on shifting trends in spatiotemporal distribution of nutrients (TN and TP), eutrophication and vulnerability to algal growth in XXB, especially during post upstream cascade reservoirs stage, are required to be investigated. Based on these findings, remedial measures to increased nutrient loading and deteriorated water quality following undesired patterns could be pointed out to ensure socio-economic objectives of reservoir and tributaries are being met.

The contributions to these tasks include the following: (1) establishment of a 2-D CEQUAL-W-2 hydrodynamic and water quality model of XXB for 11 years; (2) modelling and simulation of reflective density current patterns in collaboration with water quality variables like TN, TP etc.; (3) elucidation of TN and TP distribution on surface during pre and post upstream cascade reservoirs stages; (4) establishing relationship of nutrients distribution with shifts in effective and ineffective water circulation patterns; and (5) declaration of nutrients threats if alarming, dangerous or acceptable in terms of vulnerability to algal growth. Based on these variations, susceptibility of XXB to algal growth and countermeasures could be predicted.

## 2. METHODS

### 2.1. Research area

The TGR, caused by the Three Gorges Dam between Chongqing and Yichang (China), is among the largest in the world, with a water level of 175 m ASL, a storage capacity of $3.93 \times 10^{10}$ L, watershed area of over $1.00 \times 10^{6}$ km$^2$ and surface area range of 1080 km$^2$ (Chuo *et al.* 2019). The XXR is the major tributary in the lower reach of the TGR and is perceived as reflective of other eutrophic tributary bays of the TGR (Ji *et al.* 2017; Li *et al.* 2020b). It occupies a watershed area of 3095 km$^2$ with an average discharge of 47.4 L/s per year and a peak value of 300 L/s (Jin *et al.* 2019). It ranges from 110 °25′ E to 111 °06′ E to 30 °57′ N to 31 °34′ N as shown in Figures 1(a) and 1(b). The inceptive filling of the TGR in June, 2003 to 135 m has submerged 24 km by backwater extension, that led to formation of a huge Xiangxi bay. The backwater upstream transgression is almost 40 km once the TGR was filled to the maximum water level (175 m) (Jin *et al.* 2019).

The mainstream of Xiangxi River (XXR) is approximately 94 km long. Its water shed is elevated from 1200 to 2000 m including Xingshan County, Zigui County and wedges of the Shennongjia Forest, occupying a total area of 3099 km$^2$ (Li *et al.* 2019) as in Figures 1(a) and 1(b). The Xiangxi Estuary is located 34.5 km upstream from the TGD.

### 2.2. Hydrodynamic model

The CE-QUAL-W2 model is a 2D (longitudinal and vertical), laterally averaged, hydrodynamic and water quality model (Cole & Wells 2013). The model can precisely simulate thermal distribution, hydrodynamic features, and water quality parameters for different water bodies and under extensively varied conditions (Bowen & Hieronymus 2003; Ma *et al.* 2015; Chuo *et al.* 2019; Costa *et al.* 2019). The CE-QUAL-W2 model was applied for this study because of morphological suitability of XXB. Density driven currents are simulated in the model by evaluating the equation of state, which established correlation among density, concentration of dissolved substances and temperature (Saadatpour *et al.* 2017; Shabani *et al.* 2017) as shown in the

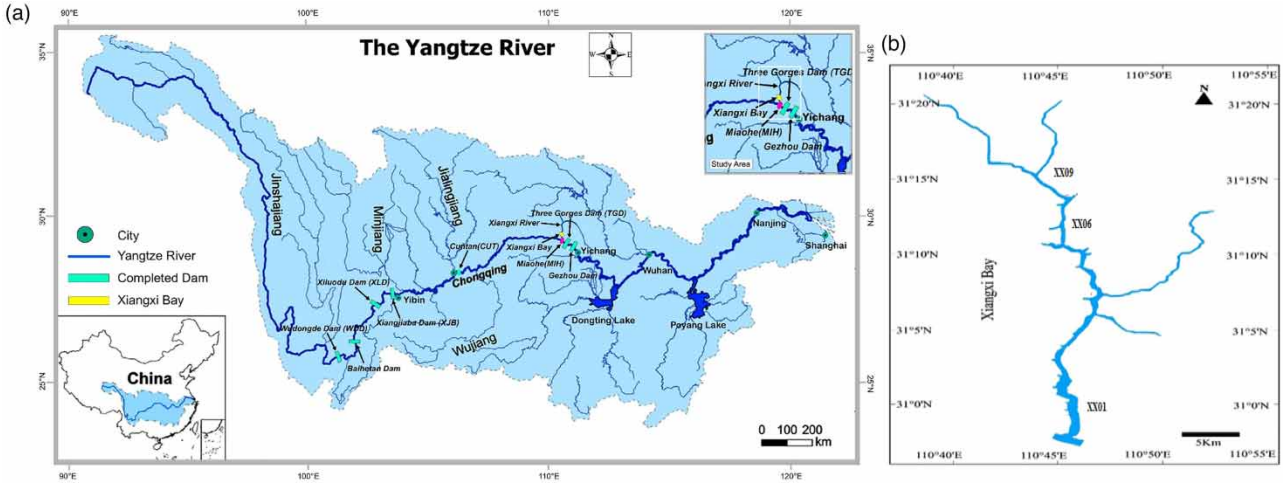


**Figure 1** | (a) Map of upstream dams and Three Gorges Reservoir (TGR) on Yangtze River, China and position of Xiangxi Bay; (b) Map of the Xiangxi Bay in the TGR.

Supplementary Data. Monthly sequence statistics, evolutionary mechanisms and shifting trends of density current patterns over seasonal and yearly scales at the mouth and end of XXR were evaluated from model simulations.

The length-to-width ratio of the XXB is almost 400, which confirms the suitability of adopting the laterally averaged CE-QUAL-W2 model. Bathymetric and geometric data of the reservoir was processed to prepare a computational grid of the XXB. This bathymetry for XXB was reflected by 64 longitudinal segments ranging from 500 to 1000 m in length. The vertical alignment includes 109 vertical layers and extends to 1 m in thickness. The model has undertaken the varying widths ranging from 20 to 1300 m. The simulation period was undertaken from January 1, 2008 to December 31, 2018. An auto-stepping algorithm in the model had processed the numerical stability parameter to find the maximum time step. Variable time steps adopted in the simulations were a divided part of this maximum time step. The initial conditions, boundary conditions, model simulations and Tecplot files are demonstrated in the Supplementary Data.

The daily inflow rate ($Q_{in}$) and inflow temperature ($T_{in}$) were established as the upstream boundary conditions for the XXB model. The daily water level (WL) and daily measured temperature ($T_{dh}$) were incorporated as the downstream boundary conditions. Meteorological data including wind velocity, air and dew point temperature and cloud cover (total incident solar radiations), were attained from the hydrological station at the upstream of the Xiangxi bay. Moreover, the initial WL in the computational domain was specified by field. The simulations of CE-QUAL-W2 model were verified by Ma *et al.* (2015) and Ijaz *et al.* (2022) and found to be in agreement with field measurements of temperature, velocity and circulation scenarios in the XXB.

### 2.2.1. CE-QUAL-W2 model functions and features

The model was chosen in this study for the following reasons:

(1) Modelling of hydrodynamics in two dimensions could accomplish both longitudinal and vertical thermal profiles and circulation patterns with respect to density current patterns.
(2) The CE-QUAL-W2 model has six unknowns with associated solution by six equations such as water surface elevation, pressure, horizontal velocity, vertical velocity, density and temperature as shown in Figure 2. Equations make good correlations among all hydrodynamic parameters.
(3) The CE-QUAL-W2 model is best suited for relatively long and narrow water bodies like XXB of TGR.
(4) FORTRAN and ULTIMATE were used as the computer language and numerical transport scenario, respectively. The FORTRAN code could be modified.
(5) Hydrodynamic mixing is modeled more accurately than with a one-dimensional or a three-dimensional model.

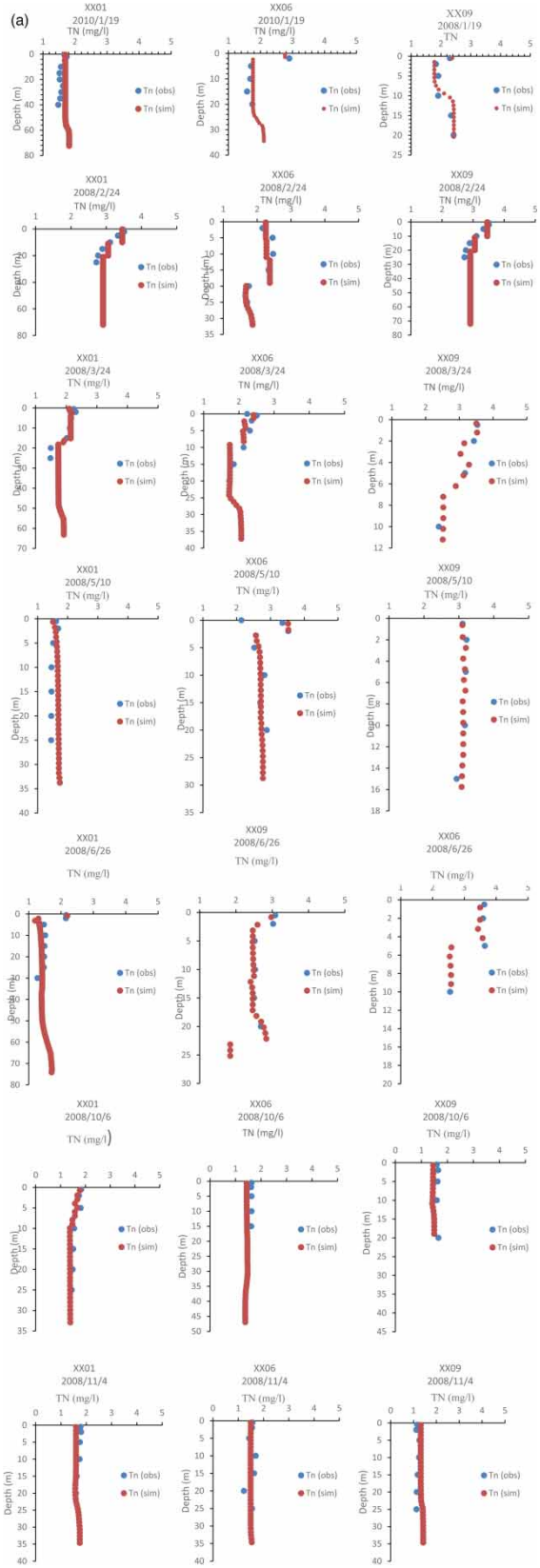


**Figure 2** | (a) Observed and simulated vertical profiles of TN at sites XX01, XX06, XX09; (b) Observed and simulated vertical profiles of TP at sites XX01, XX06, XX09. *(continued)*.

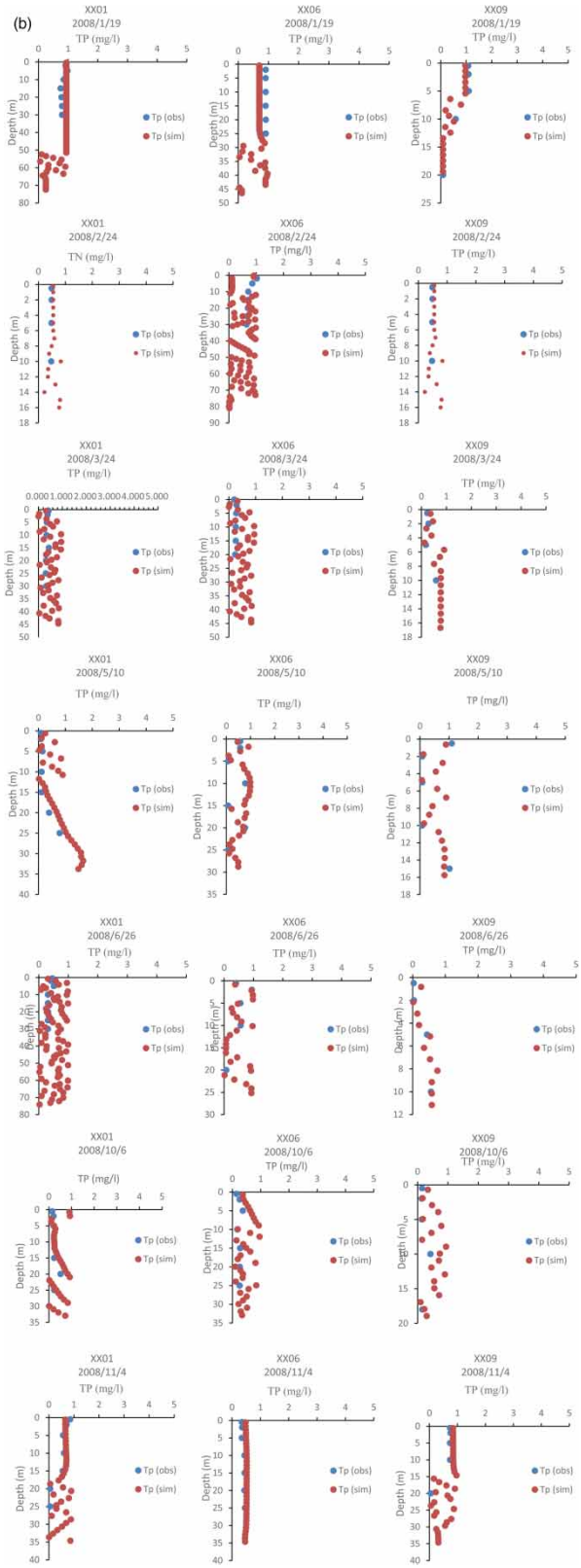


**Figure 2** | (*Continued*).

### 2.2.2. Simulation of water quality variables

Water quality variables, such as TN and TP in entire periods and stages were simulated at different reaches of XXB for 11 years. Furthermore, plots of TP and TN were depicted in figures. In this study, the W2 model was used for the simulation of water quality and eutrophication status with respect to density current patterns. These outputs could contribute in effective management techniques for controlling nutrient loading. The boundary conditions for the water quality model include inflow concentrations of $PO_4$, $NH_4$, $NO_3$, $SIO_2$, $ALG_1$, $ALG_2$, $ALG_3$, $ALG_4$, $ALG_5$, DO and nutrient concentrations at the downstream boundary. Heterogenous nutrient sources are required to be comprehended for sustainable water quality in XXB. The water movement and mixing processes are closely related to biochemical dynamics in water column (Xia *et al.* 2018).

In W2 model applications, simulations of water quality variables are preceded by hydrodynamic variables (Xiang *et al.* 2021). The CE-QUAL-W2 model is capable of simulating 21 variables including suspended soils, total dissolved solids (or salinity), a conservative tracer, sediment, total inorganic carbon, coliform bacteria, labile and refractory dissolved oxygen matter, algae, detritus, orthophosphate or total phosphorus, total nitrogen, nitrite/nitrate, dissolved oxygen, alkalinity, pH, carbon dioxide, bicarbonate, carbonate, iron, and carbonaceous biochemical oxygen demand. It is optional to select or deselect either of these options. W2 model is exquisitely described in Cole & Wells (2013).

### 2.2.3. Model calibration and validation

Model calibration is the way of finding precision of parameters through differences between the simulated data with the observed data.

The choice of effective parameters is significant for accuracy of a numerical model. The CE-QUAL-W2 model incorporated some parameters which specify hydraulic and water quality coefficients and could be altered during the model calibration (Cole & Wells 2013; Chuo *et al.* 2019).

CE-QUAL-W2 was calibrated and validated for XXB and system performances and errors were in allowed ranges as shown in Figure 2(a) and 2(b).

### 2.2.4. Error evaluation and calibration results of water quality parameters

Water temperature and velocity are effective in shaping water circulation patterns (Ijaz *et al.* 2022).

TN and TP are very significant for defining water quality, eutrophication and susceptibility to algal blooms, and hence are required to be calibrated for declaring precision in simulated results. Figures 2(a) and 2(b) indicate the calibration results for observed and model simulated TN and TP at XX01, XX06 and XX09 in XXB.

### 2.2.5. Analysis of model performance

Model performance is assessed through the mean error (ME), the absolute mean error (AME) and the root mean square error (RMSE) statistics. The ME refers to model bias. The AME elaborates model performance as it evaluates average error in simulation results. The RMSE is statistically well-oriented and is an exact index of the average difference between observations and simulations. These equations are effectively used to evaluate the extent of synchrony between the simulated and the observed data (Cole & Wells 2013; Smith *et al.* 2014). The extent-of-synchrony statistics are obtained as follows:

$$\mathrm{ME} = \frac{\sum_{i=1}^{n} (X_{\mathrm{obs},i} - X_{\mathrm{model},i})}{n} \tag{1}$$

$$\mathrm{AME} = \frac{\sum_{i=1}^{n} |X_{\mathrm{obs},i} - X_{\mathrm{model},i}|}{n} \tag{2}$$

$$\mathrm{RMSE} = \sqrt{\frac{\sum_{i=1}^{n} (X_{\mathrm{obs},i} - X_{\mathrm{model},i})^2}{n}}, \tag{3}$$

where '$n$' is the number of observations, '$X_{obs,}$ $I$' is the value of the '$i$th' observation of parameter '$X$', and '$X_{model,i}$' is the simulated value of the '$i$th' observation of parameter '$X$'.

Calibration of the CE-QUAL-W2 model proved that simulated TN and TP were in acceptable synchrony to field measurements in the XXB as shown in Figures 3(a) and 3(b). The overall averaged mean error (ME), averaged absolute mean error (AME), and averaged root mean square error (RMSE) were 0.11, 0.15, and 0.18 mg/L respectively, at site XX01; 0.12, 0.23, and 0.31 mg/L respectively, at site XX06; and 0.11, 0.17, and 0.21 mg/L respectively, at site XX09. According to Cole & Wells (2013), the nutrients vertical profiles should have AMEs less than 0.5 mg/L and RMSEs less than 1 mg/L or less than 20% for better description of nutrients, eutrophication and algal regime. All errors are less than 20% and are in acceptable ranges declaring the model viable for XXB as shown in Figures 2(a) and 2(b).

### 2.3. Distinction of density current patterns carrying nutrients from main stream

Upstream inflow from Shennongjia forest into XXB occurs as underflow for most of the year except for a few days (Long *et al.* 2019). Water intrusion from the main stream of the TGR takes place as overflow, upper interflow, interflow, lower interflow and underflow (Long *et al.* 2019; Ijaz *et al.* 2022). These intrusion positions affect hydrodynamics and water quality in XXB in different ways. This makes nutrient concentrations and eutrophication get affected at surface. Therefore, these are considered as influential for making changes to nutrients regime in XXB and implications are extensively and comparatively investigated.

### 2.4. Quantitative analysis of spatiotemporal distribution of nutrients in XXB during typical stages

The XXB was more vulnerable to algal growth than TGR in spring due to stability in water quality and hydrodynamic parameters (Ji *et al.* 2017). Isotopic measurements in XXB of TGR have verified the origin of the major contents of nutrients from the mainstream, besides indigenous developments (Wang *et al.* 2018). Spatiotemporal nutrient loading in XXB triggered by an altered flow regime in spring across the years during pre and post upstream cascade reservoir stages are investigated here.

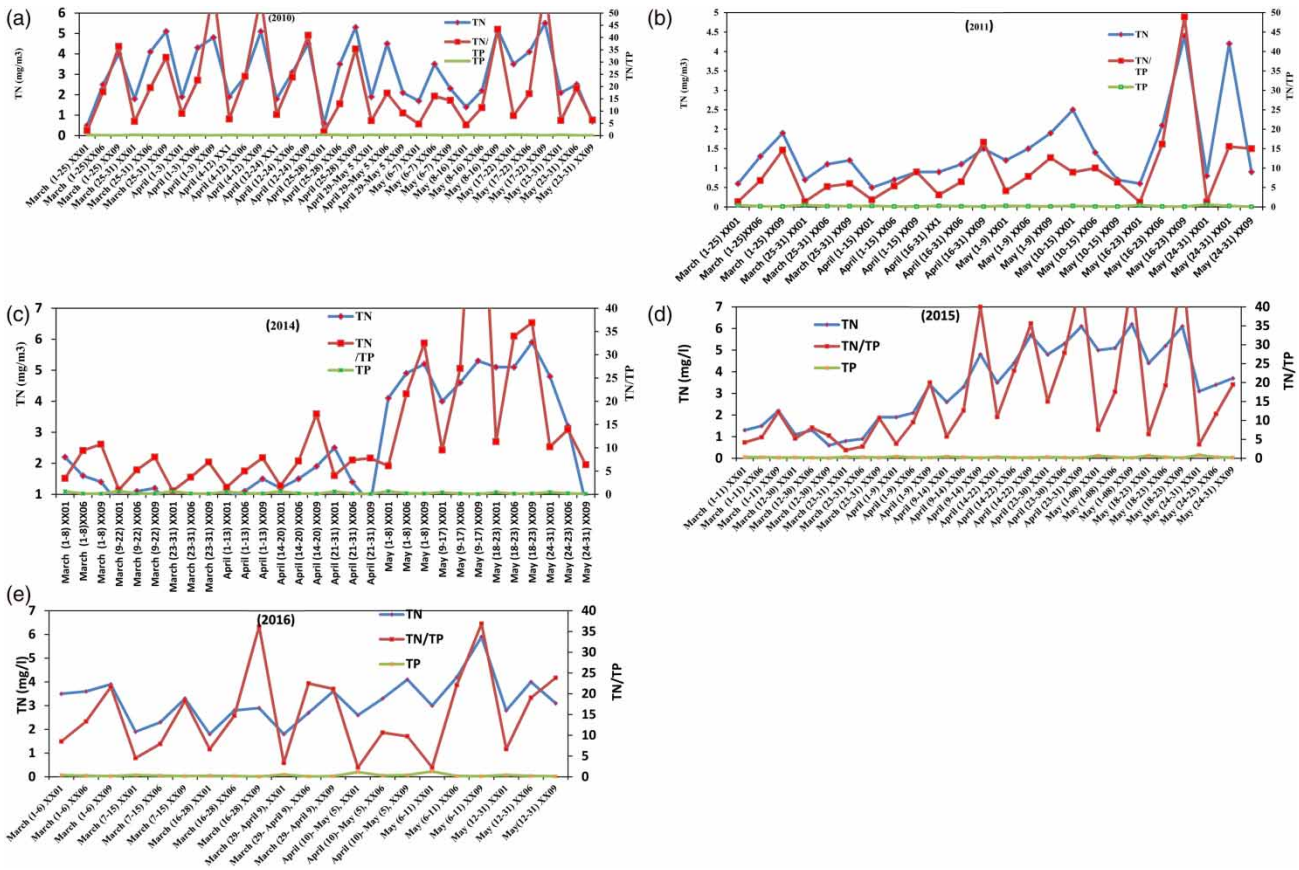


**Figure 3** | (a,b,c,d,e) Longitudinal distribution of TN,TP and TN/TP in spring from 2010 to 2016.

Furthermore, its implications were found to be significant in highlighting trophic status and vulnerability to algal regime. Subsequently, counter measures can be devised to control quality worsening. As it was found from data analysis and processing that algal growth in spring was TP limited and TN was the major nutrient responsible for eutrophication, so spatiotemporal variations in TN were thoroughly investigated and interpreted as follows.

#### 2.4.1. Longitudinal TN distribution in spring 2010

TN concentration from March 1–25 was less than 1 mg/L at 0–1000 m and 5–8 mg/L in middle and lower reaches. During late March the TN concentration in the upper reach at 0–5000 m from upstream was less than 2 mg/L, 3.8 mg/L in the middle reach at 5000–20,000 m, 4 mg/L at 20,000–22,000 m and 5–6 mg/L at 22,000–30,000 m. The TN concentration from April 1–3 at 8000 m in the upper reach was 1.9 mg/L, 3.2 mg/L at 6000–14,000 m, 5 mg/L at 14,000–20,000, 5.5 mg/L at 22,000–28,000 m and TN ranges from 6 mg/L at 28,000–31,000 m.

On April 4–12 the TN concentration in the middle reach became less than 2.7 mg/L and 3–4 mg/L in the lower reach. On April 12–24 upper and middle reaches are still less in concentration, whereas the TN concentration at 24,000–31,000 m from upstream reaches 5.8 mg/L.

On April 25–28, the TN concentration was less than 1 at 0–12,000 m, 3.1 mg/L at 12,000–20,000 m and 4–6 mg/L at 20,000–31,000 m. On April 29 to May 5, 2010, the TN concentration was less than 2.7 mg/L at 0–6000 m, 3–4 mg/L at 6000–9000 m, 4–5 mg/L at 9000–23,000 m and less than 3 mg/L in the lower reach. On May 6–7, 2010, it became less than 3 mg/L in the upper and lower reaches and 3–4 mg/L in the middle reach. On May 8–16, TN reached 1 mg/L at 6000 m in the upper reach, varying from 1–2 mg/L at 6000–10,000 m, 2–3 mg/L at 10,000–25,000 m, 6 mg/L at 26,000–31,000 m in the lower reach. On May 17–22, the upper and middle reaches had higher values of TN reaching 3.8 mg/L. On May 23–31, the TN concentration was 3 mg/L in the upper and middle reaches and was less than 1 mg/L in the lower reach.

#### 2.4.2. Longitudinal total nitrogen TN distribution in spring 2011

On March, 1–5, 2011, the TN was less than 1 at 0–24,000 m, and 1.5 mg/L at 24,000–30,000 m, On March 5–13, 2011, it was less than 1 at 0–24,000 m, 3 mg/L at 24,000–25,000 m, and 4 mg/L at 25,000–30,000 m. On March 14–20, 2011, it was less than 1 at 0–24,000 m, and 1.5 mg/L at 24,000–30,000 m.

On March 21–26, 2011, it was less than 1 mg/L at 0–21,000 m,1.5 mg/L at 21,000–26,000 m, 1.1 mg/L at 26,000–28,000 m and reduced to 0.5 mg/L at 28,000–30,000 m. On March 26–31, 2011, it was 0.8 mg/L at 0–9000 m, 1.5 mg/L at 9000–11,000 m, and 1.1 mg/L at 11,000–30,000 m, On April, 1–15, 2011, the TN was less than 1 mg/L at the upper, middle and lower reaches. On April,16–31, 2011, the TN was 1.1 mg/L at 0–14,000 m and it was 1.6 mg/L at 14,000–30,000 m. On May 1–6, 2011, the TN was 1.1 mg/L at 0–16,000 m, 1.5 mg/L at 16,000–20,000 m, 2.2 mg/L at 20,000–26,000 m and 1.5 mg/L at 26,000–30,000 m. On May 6–9, the 2011, the TN was 1.1 mg/L at 0–11,000 and 1.5 mg/L at 12,000–30,000 m. On May 9–15, 2011, the TN was 3 mg/L at 0–12,000 m, 1.1 mg/L at 12,000–26,000 m, and 0.5 mg/L at 26,000–30,000 m. On May 16–20, 2011, the TN was 0.6 mg/L at 0–26,000 m, 2.2 mg/L at 26,000–28,000 m, and 4.8 mg/L at 28,000–30,000 m. On May 21–23, 2011, the TN was 0.5 mg/L at 0–10,000 m, 1.7 mg/L at 10,000–17,000 m, 5 mg/L at 17,000–20,000 m, 7 mg/L at 20,000–21,000 m, 6 mg/L at 21,000–28,000 m and 8 mg/L at 28,000–30,000 m.

On May 24–31, 2011, the TN was 0.8 mg/L at 0–60,000 m, 1.5 mg/L at 6000–9000 m, 4.4 mg/L at 9000–12,000 m, 0.7 mg/L at 12,000–13,000 m, 4.8 mg/L at 13,000–22,000 m, 5 mg/L at 22,000–24,000 m, 1.7 mg/L at 24,000–26,000 m and 0.88 mg/L at 26,000–30,000 m.

#### 2.4.3. Longitudinal TN distribution in spring 2014

The TN concentration on March 1–8, 2014 at 0–10,000 was 4.28 mg/L, 2.50 mg/L at 10,000–15,000 m, 1.7 mg/L at 15,000–18,000 m and 1.6 mg/L at 18,000–30,000 m. The TN concentration on March 9–22, 2014 at 0–15,000 m was 1.7 mg/L and 0.7 mg/L at 15,000–30,000 m, It was 0.7 mg/L at 1–4000 m, 2.14 mg/L at 4000–21,000 m and 0.9 mg/L at 21,000–30,000 m. On March 23–25, 2014, the TN was 0.7 mg/L at 0–5000 m, 2.14 mg/L at 5000–14,000 m, 0.71 mg/L at 14,000–24,000 m and 2.14 mg/L at 24,000–30,000 m. On March 26–31, 2014 the TN was less than 0.79 mg/L at the upper, middle and lower reaches.

On April 1–13, 2014, the TN was 0.7–1.4 mg/L at 0–240,000 m from upstream and was less than 0.7 mg/L at 24,000–30,000 m. On April 14–16, 2014, the TN was 5 mg/L at 26,000–30,000 m at the lower reach. The TN on April 17–19, 2014 was 0.5 mg/L at 0–5000 m, and 1.42 mg/L at 5000–30,000 m. The TN on March 20–22, 2014 was 0.6 mg/L at 0–8000 m, 2.0 mg/L at 8000–18000 m, 2.8 mg/L at 18000–24,000 m and 4.24 mg/L at 24,000–30,000 m. On April 23–31, 2014, the TN increased to 5.0 mg/L at the upper reach.

On May 1–8, 2014 the TN was 4.8 mg/L at 0–6000 m and 4.8–5.5 mg/L at 3000–6000 m. On May 9–17, 2014, the TN was 4.5 mg/L at 0–5000 m, 5–6 mg/L at 5000–14,000 m and 4–6 mg/L at 15,000–30,000 m. On May, 18–23, 2014 the TN was 6–6.5 mg/L at the upper, lower and middle reaches. On May 24–27, 2014 the TN was 6.5 mg/L at 0–20,000 m, 4–4.5 mg/L at 20,000–23,000 m and 0.45–0.5 mg/L at 23,000–30,000 m. On May, 28–31, 2014 the TN was 5–6 mg/L at 0–3000 m, 4–5 mg/L at 3000–9000 m,5 m,5 mg/L at 9,000–11,000 m, 3.9 mg/L at 11,000–14,000 m and 0.5 mg/L at 14,000–30,000 m.

#### 2.4.4. Longitudinal total nitrogen TN distribution in spring 2015

On March, 1–5, 2015, the TN was less than 1.3 mg/L at 0–4000 m,1.0 mg/L at 4000–5000 m,1.3 mg/L at 5000–24,000 m, 1.6 mg/L at 24,000–28,000 m and 2.3 mg/L at 28,000–30,000 m. On March, 6–11, 2015 the TN was 1 mg/L at 0–7000 m, 2.0 mg/L at 7000–10,000 m, and 2.3 mg/L at 10,000–30,000 m. On March, 12–28, 2015 the TN was 1.33 mg/L at 0–5000 m, 1.0 mg/L at 5,000–21,000 m, and 0.66 mg/L at 21,000–30,000 m. On March 29–31, 2015, it was 1 mg/L at 0–6000 m, 0.66 mg/L at 6000–22,000 m, and 0.33 mg/L at 22,000–30,000 m. On April 1–3, 2015 the TN was 1 mg/L at 0–6000 m, 0.66 mg/L at 6000–23,000 m, and 0.33 mg/L at 23,000–30,000 m. On April 4–7, 2015 the TN was 2.33 mg/L at 0–3000 m, 1.6 mg/L at 3000–15,000 m, 2.0 mg/L at 15,000 m–20,000 m, 2 mg/L at 20,000–22,000 m, 2.33 mg/L at 22,000–24,000 m and 4.00 mg/L at 24,000–30,000 m. On April 7–9, 2015 the TN was 2.8 mg/L at 0–11,000 m, 3.3 mg/L at 11,000–12,000 m, 5 mg/L at 12,000–20,000 m and 5.3 mg/L at 22,000–30,000 m. On April 10–14, 2015 the TN was 4.4 mg/L at 0–4000 m and 5.8 mg/L at 7000–30,000 m. On April 15–22, 2015 the TN was 4.5 mg/L at 0–10,000 m, 5.2 mg/L at 10,000–28,000 m and increased at 28,000–30,000 m reaching 6.2 mg/L. On April 23–27, 2015 the TN was 5.5 mg/L at 0–5000 m at 6 mg/L at 5000–30,000 m. On April 28 to May 2, 2015 the TN was 5.8 mg/L at 0–14,000 m, 5.5 mg/L at 14,000–25,000 m and 6.1 mg/L at 25,000–30,000 m. On May, 3–8, 2015 the TN was 4.6 mg/L at 0–4000 m, 5 mg/L at 4000–6000 m, 5.5 mg/L at 7000–30,000 m.

On May 9–17, 2015 the TN was 4.4 mg/L at 0–15,000 m, 2.5 mg/L at 15,000–17,000 m, 2.2 mg/L at 17,000–19,000 m, and 1.1 mg/L at 19,000–30,000 m. On May 18–23, 2015 the TN was 2.2 mg/L at 0–2000 m, 4.4 mg/L at 2000–10,000 m, 3 mg/L at 10,000–18,000 m and 2.2 mg/L at 18,000–30,000 m. On May 24–31, 2015 the TN was 2 mg/L at 0–2000 m, 2.5 mg/L at 2000–3000 m, 2.3 mg/L at 3000–5000 m, 2 mg/L at 6000–11,000 m, 133 mg/L at 11,000–18,000 m and 2 mg/L at 18,000–30,000 m.

#### 2.4.5. Total nitrogen TN distribution in spring 2016

On March 1–6, 2016 the TN was 4 mg/L at 0–19,000 m, 4 mg/L at 19,000–22,000 m, 2.89 mg/L at 22,000–24,000 m and 4 mg/L at 24,000–30,000 m. On March 7–15, 2016 the TN was 1.9 mg/L at 0–10,000 m, 2.8 mg/L at 10,000–28,000 m and 3.3 mg/L at 28,000–30,000 m. On March 16–27, 2016, the TN was 1.8 mg/L at 0–4,000 m, 2.9 mg/L at 4000–21,000 m, 3.8 mg/L at 21,000–24,000 m and 3.9 mg/L at 24,000–30,000 m.

On March 28, to April 8, 2016 the TN was 1.9 mg/L at 0–10,000 m, 2.9 mg/L at 10,000–26,000 m and 3.9 mg/L at 26,000–30,000 m. On April 9 to May 5, 2016, the TN was 2.33 mg/L at 0–1000 m, 3.9 mg/L at 1000–10,000 m, 4.1 mg/L at 10,000–12,000 m and 4.5 mg/L at 12,000–30,000 m.

On May 5–11, 2016, the TN was 3 mg/L at 0–10,000 m, 3.8 mg/L at 10,000–20,000 m, 4.8 mg/L at 20,000–22,000 m, 4.6 mg/L at 22,000–24,000 m, 6 mg/L at 24,000–28,000 m and 4.3 mg/L at 28,000–30,000 m.

On May 12–31, 2016, the TN was 2.89 mg/L at 0–8000 m, 4.33 mg/L at 8000–10,000 m, 4.1 mg/L at 10,000–12,000 m, 4.8 mg/L at 12,000–20,000 m, 4.5 mg/L at 20,000–22,000 m, 4.6 mg/L at 22,000–26,000 m, 2.1 mg/L at 26,000–28,000 m and 3.33 mg/L at 28,000–30,000 m. Therefore, TN is beyond the eutrophication index, especially during late April to mid May, but it is relatively less at lower reach in late May due to more mixing in recent years.

## 3. RESULTS

### 3.1. Shifting trends in nutrient longitudinal distribution and limitation factor in spring

TN and TP distribution in the eutrophic zone is considered to be important of the indicators to algal blooms, hence shifting trends in TN, TP and TN/TP concentration determine limitation factor and changes in vulnerability of XXB to algal growth. Although the TN concentration remains high and beyond threat level, it underwent fluctuations due to shifting trends in circulation patterns and anthropogenic activities.

The simulation outcomes of TN spatiotemporal distribution of TN in XXB at the upper reach including XX01, middle reach including XXO6 and lower reach including XX09 are displayed in Table 1.

It is quite clear that average values of TN and TP differ during typical years, 2010–2011 (referring to pre-cascade dams stage) and 2014–2016 (referring to post-cascade dams stage).

**Table 1** | TN longitudinal distribution (mg/L) on surface in spring 2010–2016

**2010 Average total nitrogen (TN $_{avg}$)**

| Late March | | | Early April | | | Mid-April | | | Late April | | | Early May | | | Mid May | | | Late May | | |
|---|---|---|---|---|---|---|---|---|---|---|---|---|---|---|---|---|---|---|---|---|
| TN $_{(avg)}$ | | | TN $_{(avg)}$ | | | TN $_{(avg)}$ | | | TN $_{(avg)}$ | | | TN $_{(avg)}$ | | | TN $_{(avg)}$ | | | TN $_{(avg)}$ | | |
| UR | MR | LR | UR | MR | LR | UR | MR | LR | UR | MR | LR | UR | MR | LR | UR | MR | LR | UR | MR | LR |
| 0.4 | 2.1 | 3.1 | 1.8 | 2.9 | 3.8 | 2 | 2.9 | 4.2 | 1 | 3.8 | 4.9 | 1.9 | 4.1 | 2.7 | 1.9 | 3.1 | 4.8 | 2.1 | 2.5 | 3 |

**2011 TN $_{(avg)}$**

| Late March | | | Early April | | | Mid-April | | | Late April | | | Early May | | | Mid May | | | Late May | | |
|---|---|---|---|---|---|---|---|---|---|---|---|---|---|---|---|---|---|---|---|---|
| UR | MR | LR | UR | MR | LR | UR | MR | LR | UR | MR | LR | UR | MR | LR | UR | MR | LR | UR | MR | LR |
| 1.5 | 1.1 | 0.4 | 0.5 | 0.6 | 0.1 | 1.1 | 1.1 | 1.6 | 1.1 | 1.1 | 1.6 | 4 | 1.1 | 0.5 | 0.6 | 2.2 | 5 | 0.5 | 3.5 | 5.1 |

**2014 TN $_{(avg)}$**

| Late March | | | Early April | | | Mid-April | | | Late April | | | Early May | | | Mid May | | | Late May | | |
|---|---|---|---|---|---|---|---|---|---|---|---|---|---|---|---|---|---|---|---|---|
| UR | MR | LR | UR | MR | LR | UR | MR | LR | UR | MR | LR | UR | MR | LR | UR | MR | LR | UR | MR | LR |
| 1 | 2.1 | 2.14 | 1.2 | 1.4 | 0.7 | 1 | 2.54 | 4.5 | 2.2 | 3.3 | 4.9 | 2.5 | 5 | 5.1 | 2.8 | 4.3 | 5 | 3.5 | 5.3 | 1.9 |

**2015 TN $_{(avg)}$**

| Late March | | | Early April | | | Mid-April | | | Late April | | | Early May | | | Mid May | | | Late May | | |
|---|---|---|---|---|---|---|---|---|---|---|---|---|---|---|---|---|---|---|---|---|
| UR | MR | LR | UR | MR | LR | UR | MR | LR | UR | MR | LR | UR | MR | LR | UR | MR | LR | UR | MR | LR |
| 1.3 | 1.5 | 1.6 | 1.9 | 1.0 | 2.0 | 3 | 4.9 | 5 | 3.7 | 4.1 | 4.9 | 4 | 4.8 | 5 | 3.2 | 3.5 | 3.6 | 2.5 | 2.3 | 2 |

**2016 TN $_{(avg)}$**

| Late March | | | Early April | | | Mid-April | | | Late April | | | Early May | | | Mid May | | | Late May | | |
|---|---|---|---|---|---|---|---|---|---|---|---|---|---|---|---|---|---|---|---|---|
| UR | MR | LR | UR | MR | LR | UR | MR | LR | UR | MR | LR | UR | MR | LR | UR | MR | LR | UR | MR | LR |
| 1.9 | 2.8 | 3.2 | 2.1 | 2.7 | 2.0 | 2.9 | 2.8 | 3.4 | 2.8 | 3.7 | 4.2 | 3 | 4.2 | 5.4 | 2.89 | 4.8 | 4.9 | 2.8 | 2.6 | 2.3 |

Statistical variations in average values are stated below and are depicted in Table 1 and Figures 3(a)–3(e) and 4(a) and 4(b), which refer to the increase in TN during post dams stages, the reasons and mechanisms are discussed in the forthcoming discussion section.

The highest TN concentration at the upper, middle and lower reaches during April and May was 4, 7.8 and 8.6 mg/L respectively by 2013. The average TN concentration at the upper, middle and lower reaches during April was 1.9, 3.5 and 4.6 mg/L respectively by 2013. The average TN concentration at the upper, middle and lower reaches during May was 2, 3.8 and 5 mg/L respectively by 2013.

Overflow intrusion increased by 30% in spring and 22% in summer during post-upstream cascade reservoirs stage and have improved TN supply and distribution at the euphotic zone. TN concentration was beyond danger limit sustaining and prolonging eutrophication status in spring. The highest TN concentration at the upper, middle and lower reaches during April was 3.7, 7.7 and 9 mg/L respectively since 2014. The highest TN concentration at the upper, middle and lower reaches during May was 3.3, 7.3 and 9.2 mg/L respectively since 2014. The average TN concentration at the upper, middle and lower reaches during April was 2.1, 3.7 and 4.8 mg/L respectively since 2014. The average TN concentration at the upper, middle and lower reaches during May was 1.9, 3.4 and 4.5 mg/L respectively since 2014.

Highest total nitrogen (HTN) in XXB in spring decreased at the upper and middle reaches by 1 and 4% and fluctuated at the lower reach, since 2014. This decrease in maximum limit refers to enhanced prevalence of overflow intrusion and hydrodynamical changes like less water age and more mixing (Ijaz *et al.* 2022). Average (TN) increased at the upper, middle and lower reaches by 3, 5 and 11% respectively due to maximum supply from main stream and more water exchange followed by

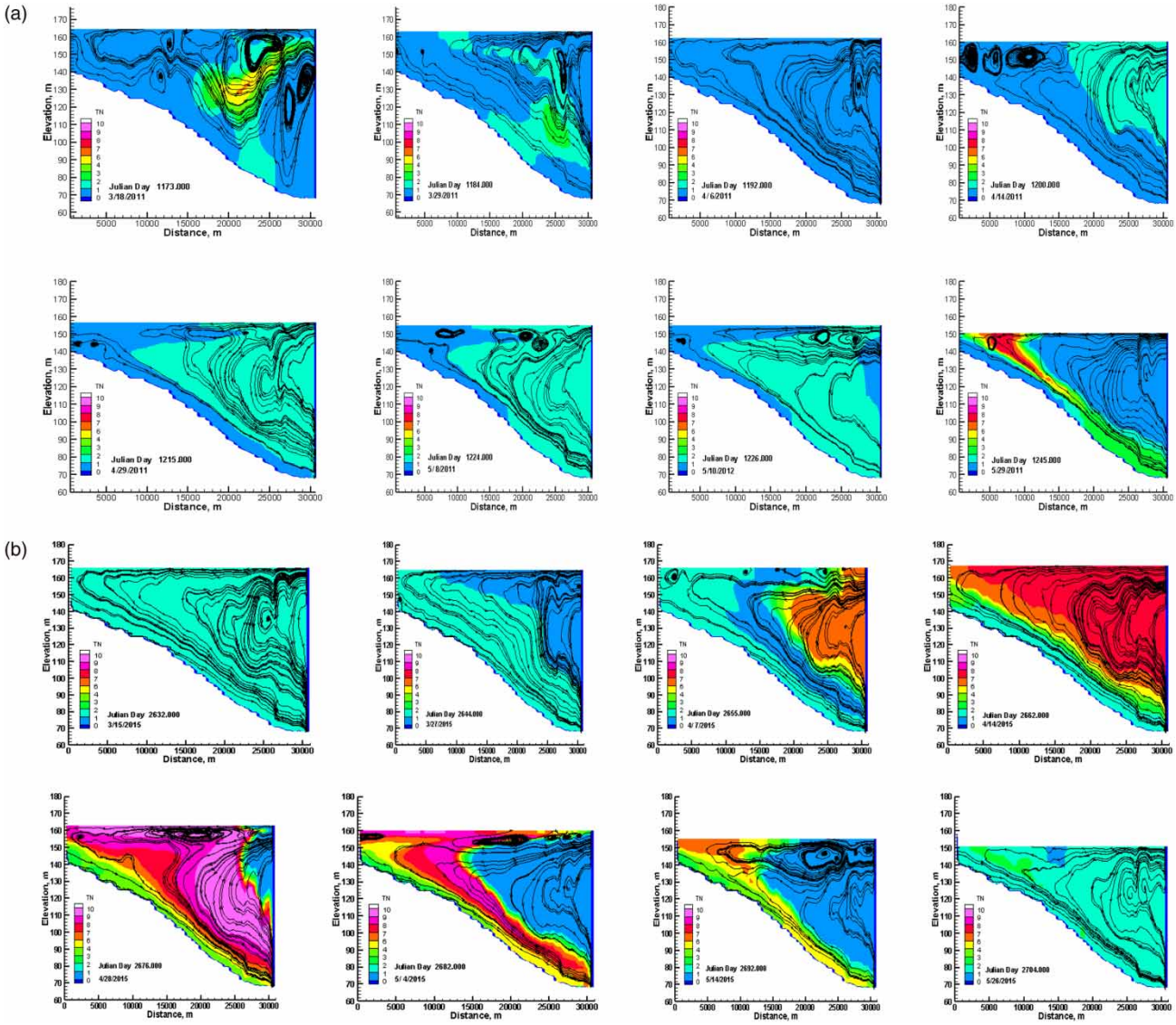


**Figure 4** | (a) Spatiotemporal dynamics trend in TN corresponding to different patterns in spring 2011; (b) Spatiotemporal dynamics trend in TN corresponding to different patterns in spring 2015.

increased overflow intrusion and increased anthropogenic activities. Average TN fluctuated at lower reach in a complicated way in May since 2014, as it increased initially in early May and decreased in late May due to prolonged overflow intrusion. The less comparative TN by 2013 reflects less supply from mainstream and less water exchange and speed on surface.

Although TP concentration in spring also fluctuated at the upper, middle and lower reaches over the years, average values remain less than 0.5 and 0.3 mg/L at the middle and lower reaches. TP was higher (0.92 mg/L) at upstream at XX01 over the entire period as upstream was the major supplier. TP also fluctuated by 1% at the lower reach since 2014.

Eutrophication and algal growth in XXB remained TP limited over the entire period with few exceptions at the upper reach. Although TP increased at the lower reach, eutrophication remained TP limited for most of the cases with a few exceptions.

Average TN increased by 0.1, 0.3 and 0.5 mg/L at the upper, middle and lower reaches respectively in Late March since 2014 compared to those in early years. It increased by 0.2, 0.7 and 0.8 mg/L at the upper, middle and lower reaches in early April since 2014. It increased by 0.3, 0.6, and 0.9 mg/L at the upper, middle and lower reaches in mid April since 2014. It increased a bit at the upper reach, 0.6 mg/L at the middle reach and 1.9 mg/L at the lower reach during late

April. In early May, it increased a bit at the upper reach, by 0.7 mg/L at the middle reach and by 0.8 mg/L at the lower reaches corresponding to either of the patterns. During mid May, it remained the same at the upper reach, and increased by 0.2 mg/L at the middle reach and 0.5 mg/L at the lower reaches. During late May, it remained the same at the upper reach, decreased by 0.4 mg/L at the middle reach and 0.6 mg/L at the lower reaches.These statistics indicate an average increase in TN in spring except in late May as in Figure 4(a) and 4(b)).

### 3.2. TP longitudinal distribution and shifting trends in spring 2010–2016

TP concentration in spring also fluctuated at the upper, middle and lower reaches, but average values remain less than 0.5 and 0.3 mg/L at the middle and lower reaches. Average TP was higher (0.92 mg/L) at the upper reach at XX01 as upstream was a major supplier. This trend remains consistent during pre and post cascade reservoirs stages (Table 2).

### 3.3. Implications of shifts in density current patterns on TN and TP longitudinal distribution

#### 3.3.1. TN longitudinal distribution on surface from April, 17–23, 2010

TN concentration on the surface decreased at the upper (XX01) and middle (XX06) reaches from April 17–19, 2010 due to overflow intrusion. TN supply at the lower reach (XX09) was higher (4 mg/L) from the main stream on April 19, 2010. Total nitrogen (TN). The TN concentration on the surface increased by 1 mg/L on average at the upper and middle reaches including XX01 and XX06 from April 20–23, 2010 due to weak vertical mixing triggered by upper interflow intrusion as evident from Figure 5(a). Figure 5(a) indicates a decrease in TN concentration at the upper and middle reaches owing to continuity of favorable overflow, whereas it increased at the upper and middle reaches and decreased at lower reaches corresponding to continuity of upper interflow intrusion.

#### 3.3.2. TP longitudinal distribution from April, 17–23, 2010

TP concentrations at the middle and upper reaches were not affected by overflow intrusion from April 17–19, 2010 and increased by 0.8 mg/L at lower reaches as evident from Figure 5(c). TP concentration decreased at the lower reach from 1.2 mg/L on April 19, 2010, to 0.5 mg/L at 25,000–30,000 m on April 23, 2010 owing to upper interflow intrusion from April 20–23, 2010. TP concentrations at the middle and upper reaches do not get affected much due to slow speed and less vertical mixing as evident from Figure 5(c). Hence, the TP longitudinal distribution increased obviously at the lower reach following continuous favorable overflow intrusion and vice versa. Although the mainstream is not the main supplier of TP, TP was seen in some parts.

#### 3.3.3. TN longitudinal distribution from April 30 to May 10, 2010

TN on May 2, 2010 was 7.2 mg/L at 9000–22,000 m and less than 1 mg/L at the upper and lower reaches corresponding to overflow intrusion. TN increased at 20,000–30,000 m reaching 2.5 mg/L and decreased at the sensitive zone (XX06) due to less water exchange and more consumption of nutrients following continuous upper interflow intrusion from May 2–10, 2010. Low surface water velocity and weak vertical mixing were the prominent causes for nutrient enrichment on the surface at the lower reach. Hence, TN increased at the lower reach and decreased at the middle reach following upper interflow intrusion as shown in Figure 6(a) and 6(b). The mechanism behind the decrease in TN at the middle reach is less water exchange potential of intruding water.

#### 3.3.4. TP longitudinal distribution from April 30 to May 10, 2010

In general, TP does not get affected much following shifts in density current patterns as shown in Figure 6(c) and remained less or close to the eutrophication threshold limit, despite having been increased at the lower reach in the subsurface following in-depth intrusion.

#### 3.3.5. TN longitudinal distribution from June 1–14, 2010

TN on June 2, 2010 was 1.5 mg/L at 0–14,000 m and less than 1 mg/L at 14,000–30,000 m. Overflow intrusion continued from June 1–14, 2010 and TN on June 14, 2010 was 1.5 mg/L at 0–7000 m from the upper reach, and increased to 2.5 mg/L at the middle reach (7000–17,000 m), 1.3 mg/L at 17,000–20,000 m and 0.5 mg/L at 20,000–30,000 m. TN increased at the upper and middle reaches following overflow intrusion from June 1–14, 2010, as shown in Figure 7(a) and 7(b). Overflow intrusion continued and resulted in increased nutrients supply.

**Table 2** | TP longitudinal distribution (mg/L) on surface in spring 2010–2016

**Average Total Phosphorus (TP avg) in spring 2010**

| Late March | | | Early April | | | Mid-April | | | Late April | | | Early May | | | Mid May | | | Late May | | |
|---|---|---|---|---|---|---|---|---|---|---|---|---|---|---|---|---|---|---|---|---|
| UR | UR | LR | UR | MR | LR | UR | MR | LR | UR | MR | LR | UR | MR | LR | UR | MR | LR | UR | MR | LR |
| 0.44 | 0.35 | 0.32 | 0.31 | 0.20 | 0.15 | 0.25 | 0.21 | 0.17 | 0.31 | 0.27 | 0.17 | 0.32 | 0.18 | 0.17 | 0.27 | 0.20 | 0.32 | 0.20 | 0.23 | 0.22 |

**Average Total Phosphorus (TP avg) in Spring 2011**

| Late March | | | Early April | | | Mid-April | | | Late April | | | Early May | | | Mid May | | | Late May | | |
|---|---|---|---|---|---|---|---|---|---|---|---|---|---|---|---|---|---|---|---|---|
| UR | UR | LR | UR | MR | LR | UR | MR | LR | UR | MR | LR | UR | MR | LR | UR | MR | LR | UR | MR | LR |
| 0.1 | 0.1 | 0.1 | 0.1 | 0.2 | 0.1 | 0.1 | 0.2 | 0.2 | 0.7 | 0.6 | 0.4 | 0.9 | 0.5 | 0.3 | 0.8 | 0.1 | 0.2 | 0.8 | 0.3 | 0.3 |

**Average Phosphorus (TP avg) in Spring 2014**

| Late March | | | Early April | | | Mid-April | | | Late April | | | Early May | | | Mid May | | | Late May | | |
|---|---|---|---|---|---|---|---|---|---|---|---|---|---|---|---|---|---|---|---|---|
| UR | MR | LR | UR | MR | LR | UR | MR | LR | UR | MR | LR | UR | MR | LR | UR | MR | LR | UR | MR | LR |
| 0.8 | 0.34 | 0.18 | 0.7 | 0.46 | 0.32 | 0.42 | 0.28 | 0.7 | 0.4 | 0.31 | 0.32 | 0.58 | 0.28 | 0.15 | 0.46 | 0.26 | 0.21 | 0.28 | 0.20 | 0.19 |

**Average Phosphorus (TP avg) in Spring 2015**

| Late March | | | Early April | | | Mid-April | | | Late April | | | Early May | | | Mid May | | | Late May | | |
|---|---|---|---|---|---|---|---|---|---|---|---|---|---|---|---|---|---|---|---|---|
| UR | MR | LR | UR | MR | LR | UR | MR | LR | UR | MR | LR | UR | MR | LR | UR | MR | LR | UR | MR | LR |
| 0.1 | 0.3 | 0.2 | 0.8 | 1.6 | 1.4 | 1.3 | 1 | 1 | 0.6 | 0.3 | 0.2 | 0.3 | 0.29 | 0.2 | 0.2 | 0.2 | 0.19 | 0.26 | 0.17 | 0.16 |

**Average Phosphorus (TP avg) in Spring 2016**

| Late March | | | Early April | | | Mid-April | | | Late April | | | Early May | | | Mid May | | | Late May | | |
|---|---|---|---|---|---|---|---|---|---|---|---|---|---|---|---|---|---|---|---|---|
| UR | MR | LR | UR | MR | LR | UR | MR | LR | UR | MR | LR | UR | MR | LR | UR | MR | LR | UR | MR | LR |
| 0.6 | 0.4 | 0.4 | 0.78 | 0.5 | 0.3 | 0.5 | 0.4 | 0.3 | 1.0 | 0.6 | 0.3 | 1.1 | 0.6 | 0.4 | 0.4 | 0.5 | 0.3 | 0.8 | 0.6 | 0.5 |

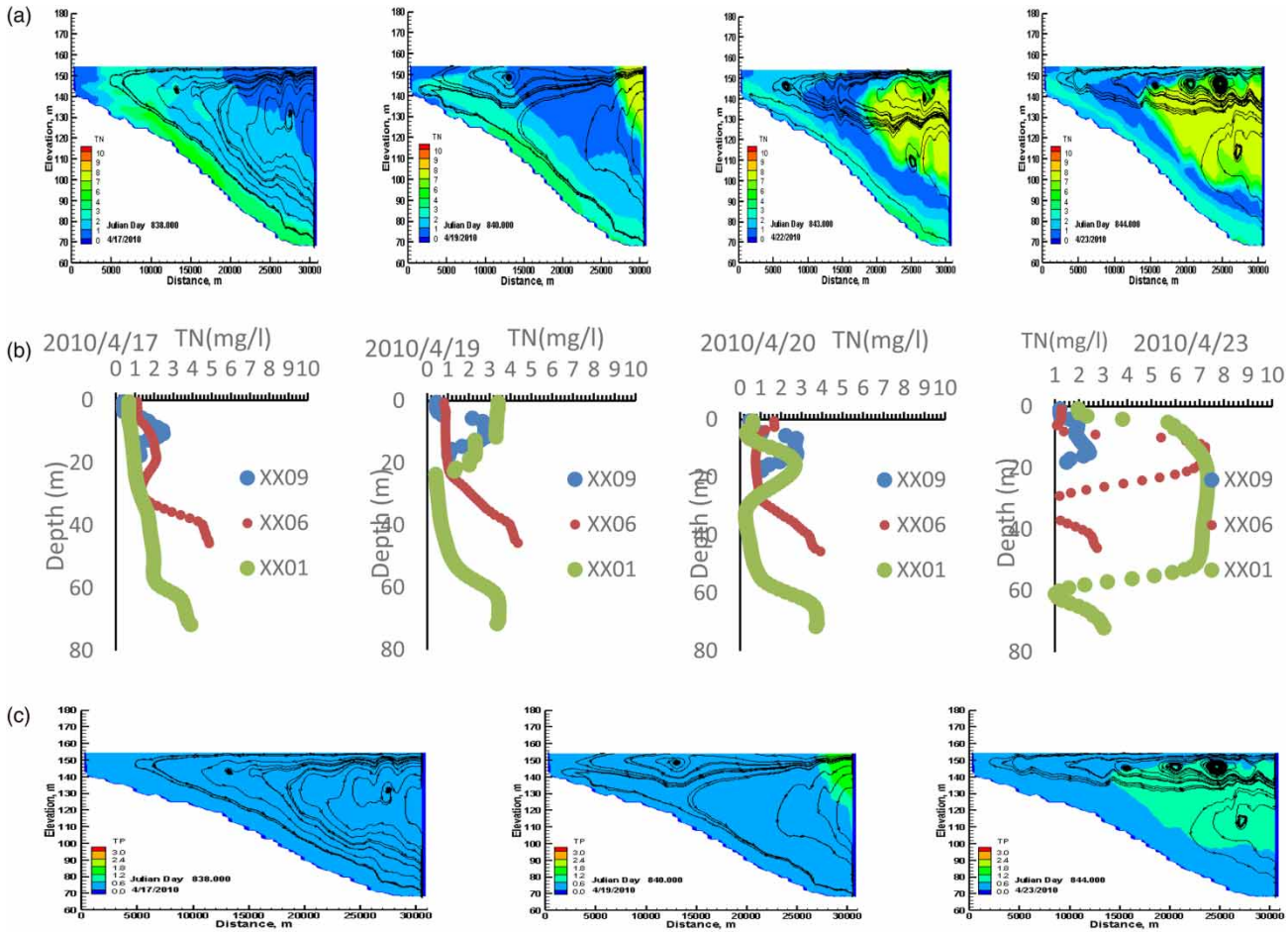


**Figure 5** | (a) Effects of shifts in density current patterns on TN longitudinal dynamics; (b) Effects of shifts in density current patterns on TN longitudinal distribution; (c) Effects of shifts in density current patterns on TP longitudinal distribution.

### 3.3.6. TP concentration from June 1 to July 3, 2010

TP was less than 0.5 mg/L during these days and was not much affected by shifting in density current patterns as shown in Figure 7(c).

### 3.3.7. TN longitudinal distribution from April 24–May 2, 2011

Overflow intrusion occurred on April 24–29, 2011, TN was decreased from 1.3 to 0.5 mg/L at the middle reach (13,000–17,000 m) and was 0.5 mg/L at 0–17,000 m and 1.30 mg/L at 17,000–30,000 m. This reflects the tendency of overflow previously existing less values of TN at the middle reach due to the potential exchange of water. Subsequently, Pattern (7) replaced Pattern (6) and continued from April 30 to May 2, 2011, and TN on May 2, 2011 was 0.7 mg/L at 0–25,000 m, and 1.2 mg/L at 25,000–30,000 m. Therefore, TN was reduced at XX06 from 1.3 to 0.6 mg/L and 1.1 from 1.6 mg/L at XX09 due to less supply on the surface, weak mixing on account of in-depth intrusion and and more consumption by proliferated algal blooms in late spring as shown in Figure 8(a) and 8(b).

### 3.3.8. TP distribution from April 24–May 2, 2011

There is no significant effect of such alterations of density currents on TP longitudinal distribution during the aforementioned days as in Figure 8(c).

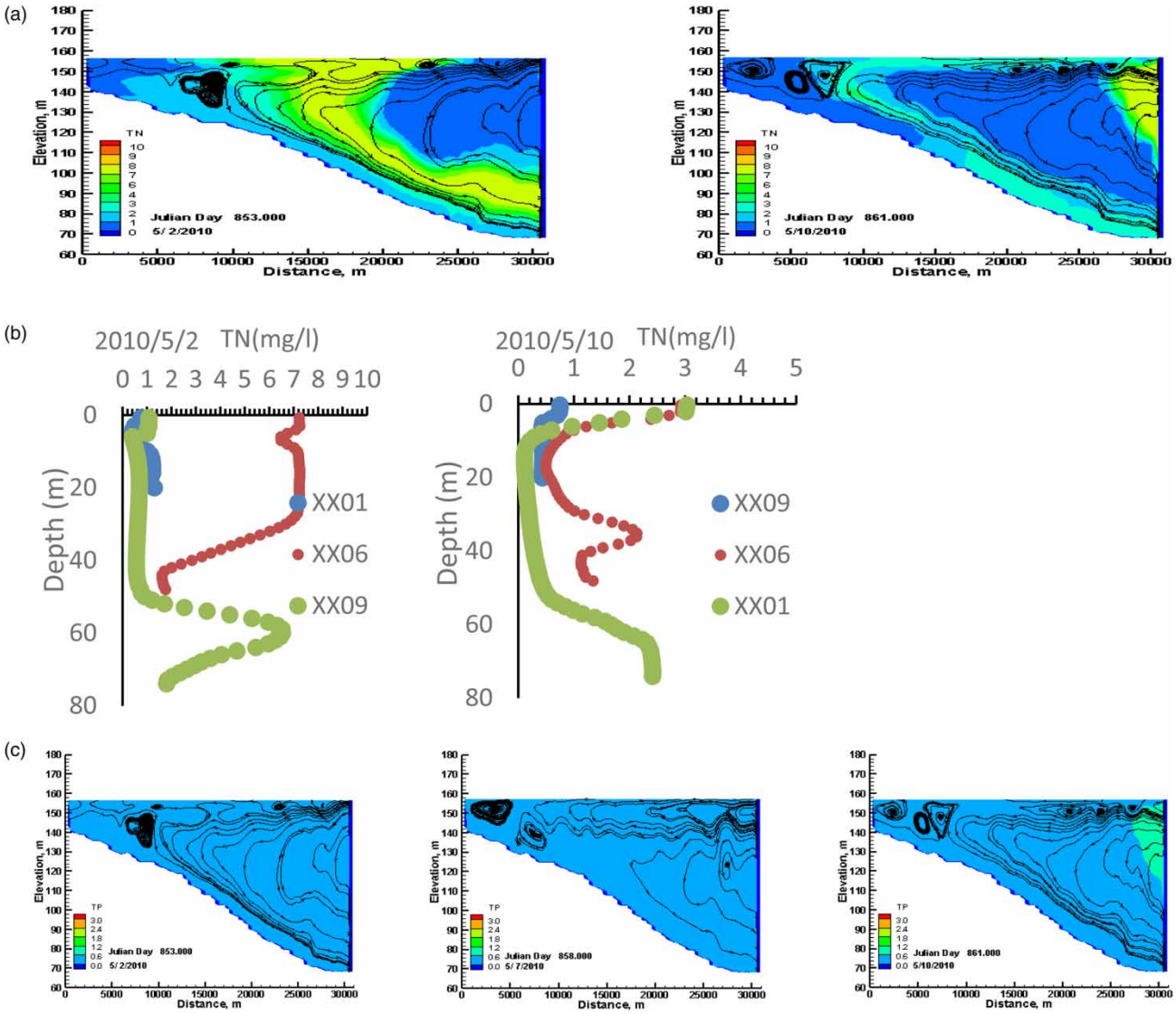


**Figure 6** | (a) Effects of shifts in current patterns on TN longitudinal distribution from April 30–May 10; (b) Effects of shifts in current patterns on TN longitudinal distribution from April 30–May 10; (c) Effects of shifts in current patterns on TP longitudinal distribution from April 30–May 10.

### 3.3.9. TN longitudinal distribution from April 21 to May 5, 2014

TN concentration on April 21, 2014 following upper interflow intrusion was 0.5 mg/L at 0–8000 m, 1.5 mg/L at 8000–23,000 m and 2.5 mg/L at 23,000–30,000 m.

As overflow intrusion continued from April 22–May 5, 2014 and TN supply on the surface kept on increasing. It was 0.5 mg/L at 0–4000 m, 1.5 mg/L at 4000–20,000 m, 2.5 mg/L at 20,000–26,000 m and 6 mg/L at 26,000–30,000 m on April 22, 2014. Similarly, TN concentration increased to 2.5 mg/L at XX01 and 6.5 mg/L at 1200–30,000 m on My 5, 2014 as shown in Figure 9(a) and 9(b). An obvious increase in TN at the upper, middle and lower reaches was observed, which made it more vulnerable to eutrophication and algal growth.

### 3.3.10. TP-concentration from April 21 to May 5, 2014

Similarly, the TP concentration was initially increased at the middle reach following overflow intrusion, but reduced on May 5, 2014 due to increased exchange and more mixing.

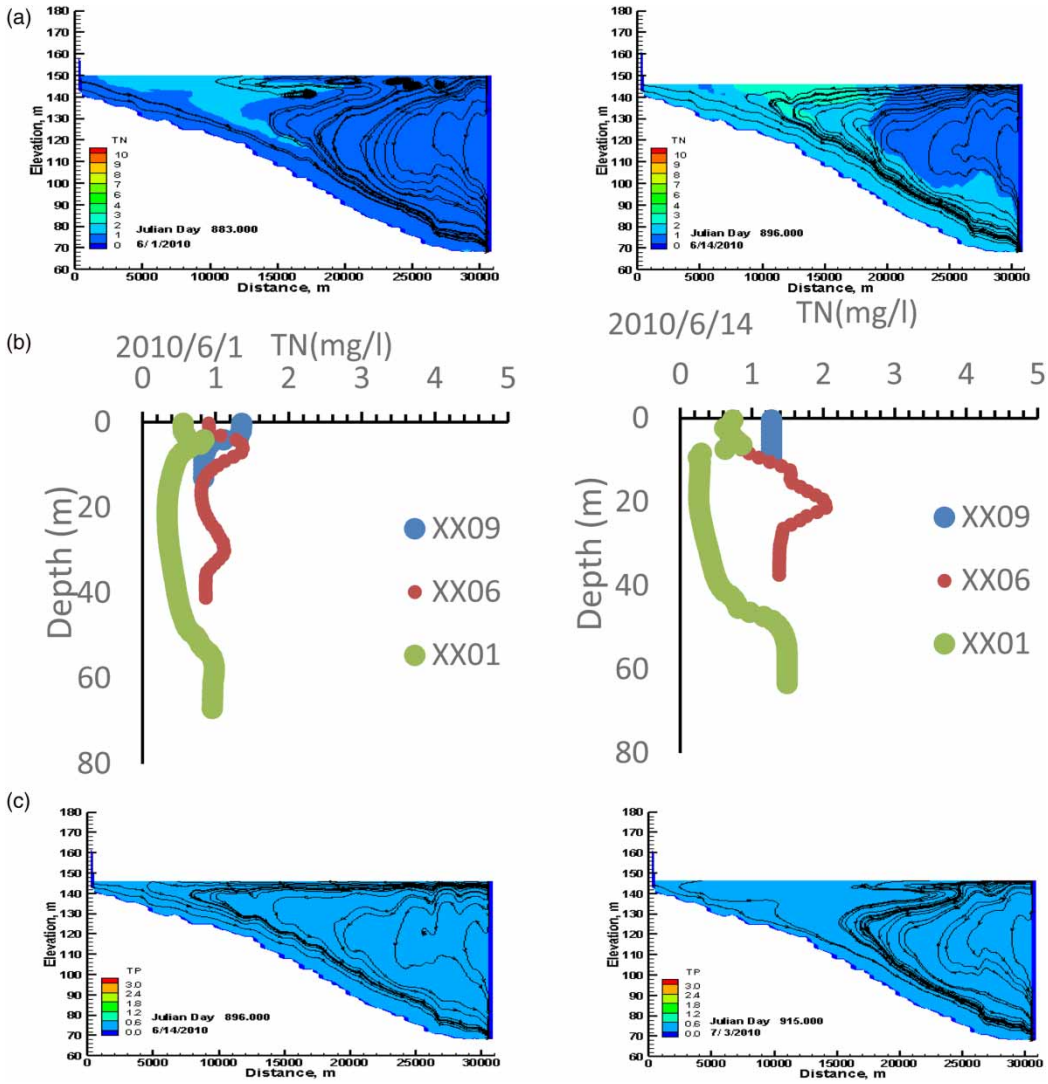


**Figure 7** | (a) Effects of shifts in current patterns on TN longitudinal distribution; (b) Effects of shifts in current patterns on TN longitudinal distribution; (c) Effects of shifts in current patterns on TP longitudinal distribution.

### 3.3.11. TN longitudinal distribution on May 7–11, 2015

Upper interflow intrusion was prevalent on May 8–11, 2015 and TN was decreased at the upper, middle and lower reaches as shown in Figure 10(a).

### 3.3.12. TP distribution from May 7–11, 2015

As algal mass in XXB in spring was TP limited, so there was no significant impact of shifts in density current patterns on TP concentration during the aforementioned days as shown in Figure 10(b).

### 3.3.13. TN longitudinal distribution on March 7–16, 2016

Interflow intrusion was prevalent on March 7, 2016 and TN was 2.9 mg/L at 0–2000 m, 3.2 mg/L at 2000–20,000 m, 3.0 mg/L at 20,000–28,000 m and 3.2 mg/L at 28,000–30,000 m. Lower interflow intrusion was prevalent on March 8–16, 2016, and TN was reduced as 2.7 mg/L at 0–2000 m, 2.9 mg/L at 2000–28,000 m and 3.1 mg/L at 28,000–30,000 m on 16 March, 2016 as in Figure 11(a) and 11(b). These statistics have validated the effectivity of lower interflow intrusion in reducing TN on the surface at the middle reach and increasing it at the lower reach. This happened on account of increased supply of nutrients at the

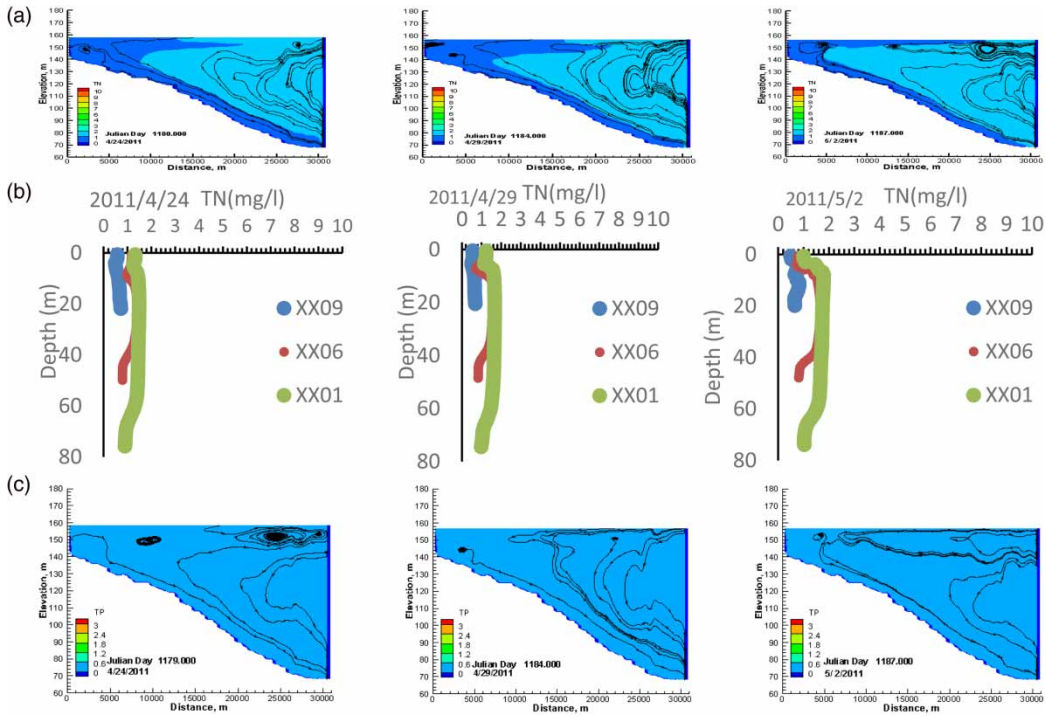


**Figure 8** | (a) Effects of shifts in current patterns on TN longitudinal distribution; (b) Effects of shifts in current patterns on TN longitudinal distribution; (c) Effects of shifts in density currents on TP longitudinal distribution from April 24 to May 2, 2011.

lower reach due to clockwise circulation of intruding water and less supply at the middle and upper reaches as shown in Figure 11(a) and 11(b). Therefore, shifting among patterns is impactful to TN concentration either way.

#### 3.3.14. TP from March 7–16, 2016

Interflow intrusion was prevalent on March 7, 2016 and TP was 1.2 mg/L at the upper, middle and lower reaches. Lower interflow intrusion was prevalent on March 8–16, 2016, and TP was 1.1 mg/L at the upper, middle and lower reaches as shown in Figure 11(c). These statistics have validated no considerable changes in TP concentration during these days.

### 3.4. Discrepancy and deviation from general principal and underlying mechanisms

Based on continuity of either of the patterns for longer time, hydrodynamic conditions are likely to be changed either in an advantageous or disadvantageous way in terms of effects on vulnerability of XXB to eutrophication and algal growth. The upcoming account elucidates exceptional cases and trends of decreased longitudinal distribution of nutrients in spite of overflow intrusion (maximum supply on surface). These variations find their basis in increased vertical mixing, less water age and fast speed on the surface following the longest continuous duration of overflow intrusion as shown in Figures 12 and 13.

#### 3.4.1. TN distribution from May 19–27, 2010

TN concentration in the lower and middle reaches was decreased from 2.5 to 0.9 mg/L at 20,000–25,000 m from upstream, due to overflow intrusion on May 20–27, 2010. This decrease in TN concentration was due to intense mixing and vertical transport of nutrients included in the intruded water.

Although nutrients contents increased initially due to overflow intrusion, they get mixed due to anticlockwise circulations and eutrophication is less likely as evident from Figure 12.

#### 3.4.2. TN longitudinal dynamics on May 23–30, 2015

Additionally, the concentration of TN also decreased on the surface, especially at the upper reach on May, 23–30, 2015 as shown in Figure 13. TN concentration was reduced from 3.5 to 2 mg/L at the upper reach and 2.8 to 1.8 mg/L at the middle reach as shown in Figure 13. TN at the upper reach was driven to mix with deep water by anticlockwise circulations

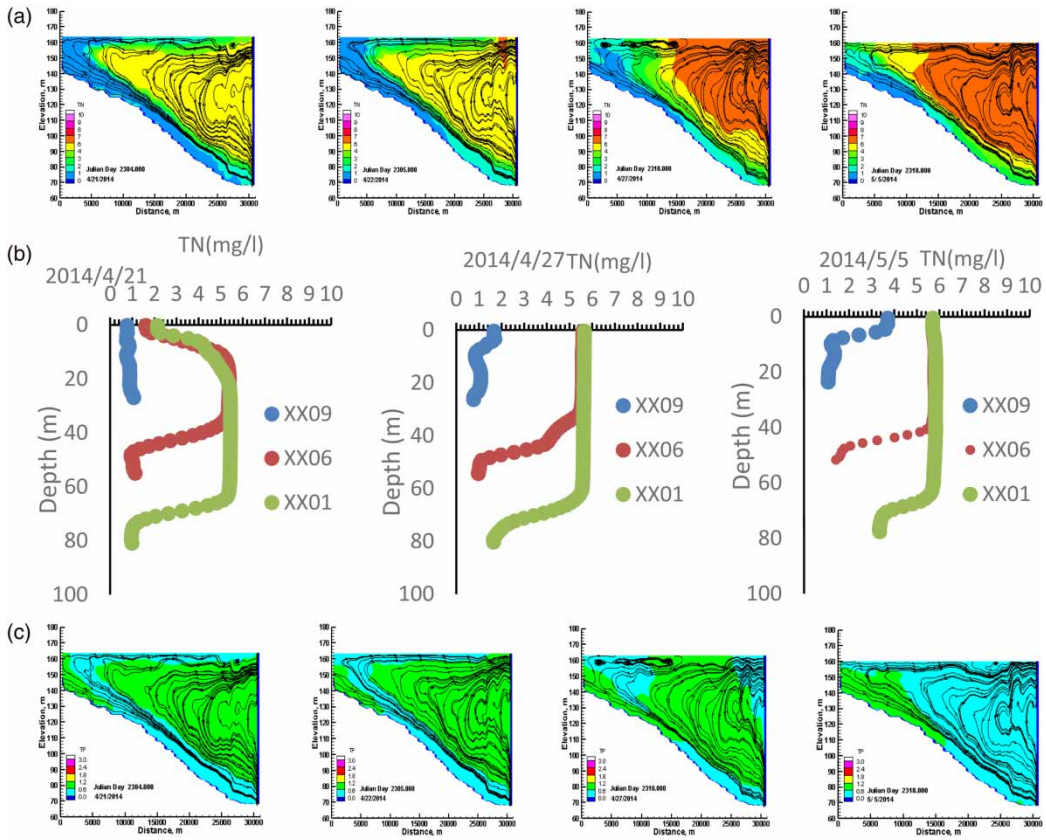


**Figure 9** | (a) Effects of shifts in current patterns on TN longitudinal distribution on April 21–May 5; (b) Effects of shifts in density current patterns on TN longitudinal distribution on April 21–May 5; (c) Effect of shift in density current patterns on TP longitudinal distribution on April 21–May 5.

resulting in substantial reduction at the upper layer, which is the most vulnerable layer in spring and is provided with enriched nutrients especially with TP. The poor TN enrichment at the upper layer corresponded to continuous mixing triggered by overflow intrusion and verified its effectivity in tackling eutrophication.

The pictorial display clearly indicates the nutrients movements and concentrations in the upper, middle and lower reaches corresponding to density current patterns. Vibrant eddies and potential water exchange corresponding to overflow revealed continuous mixing and decrease in nutrient content following the longest continuity of interflow intrusions as shown in Figures 12 and 13. As per hydrodynamic conditions, susceptibility of XXB to algal growth apparently depends on duration, continuity and frequency of density current patterns which effect eutrophic depth and mixing depth.

The upcoming account elucidates exceptional cases and trends of decreased longitudinal distribution of nutrients in spite of overflow intrusion (maximum supply on surface). These variations find their basis in increased vertical mixing, less water age and fast speed on the surface following the longest continuous duration of overflow intrusion as shown in Figure 13.

### 3.4.3. TN longitudinal distribution from June 23 to July 3, 2010

TN increased at the upper, middle and lower reaches following upper interflow intrusion on June 14–23, 2010 and was 5.5 mg/L at 0–9000 m, 7 mg/L at 9000–19,000 m and 8.2 mg/L at 19,000–30,000 m. This increase in TN refers to increased water age, less mixing and temperature stratification triggered by upper interflow. Overflow intrusion continued again from June 24 to July 3, 2010 and TN was decreased at the middle and lower reaches and was 3.5 mg/L at 0–15,000 m, 2.5 mg/L at 15,000–21,000 m, 2 mg/L at 21,000–25,000 m and 1 mg/L at 25,000–30,000 m as shown in Figure 14. This decrease in TN at the middle and lower reaches was due to the rapid movement of intruding water following overflow intrusion.

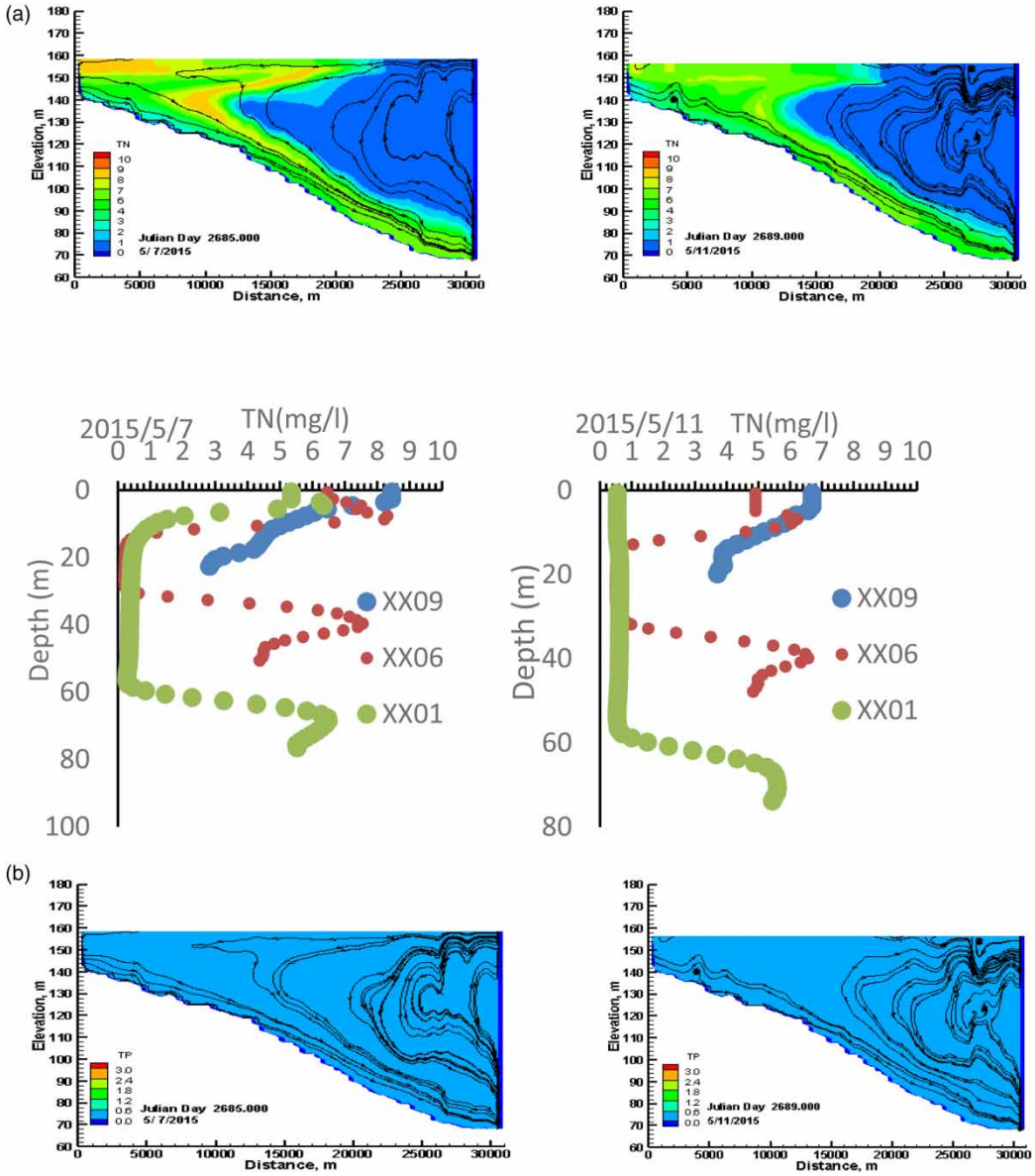


**Figure 10** | (a) Effects of shifts in current patterns on TN longitudinal concentration; (b) Effects of shifts in current patterns on TP longitudinal distribution.

## 4. DISCUSSION

### 4.1. Phenomena behind fluctuated nutrients regime during pre and post upstream cascade reservoir stages

Water quality and eco-hydrological alterations are shown to have been affected by specifications associated with varying density driven water circulation patterns (Ma *et al.* 2015). Moreover, continuity and transitions among density currents patterns have differently affected thermal structure, mixing, water age (Ji *et al.* 2017), spatiotemporal transport as well as nutrients distribution in XXB besides other ingredients, as shown in Figures 3–14. Effective density current patterns (overflow, lower interflow and underflow intrusions) for algal growth are accompanied with increased water exchange, velocity on the surface, mixing depth and intensity, and hence are supposed to cause a reduction in nutrient distribution on the surface in terms of hydrodynamical simultaneous phenomena. Conversely, ineffective patterns (upper interflow and interflow intrusions) are accompanied with decreased water exchange, more water age, less velocity on the surface, less mixing depth and

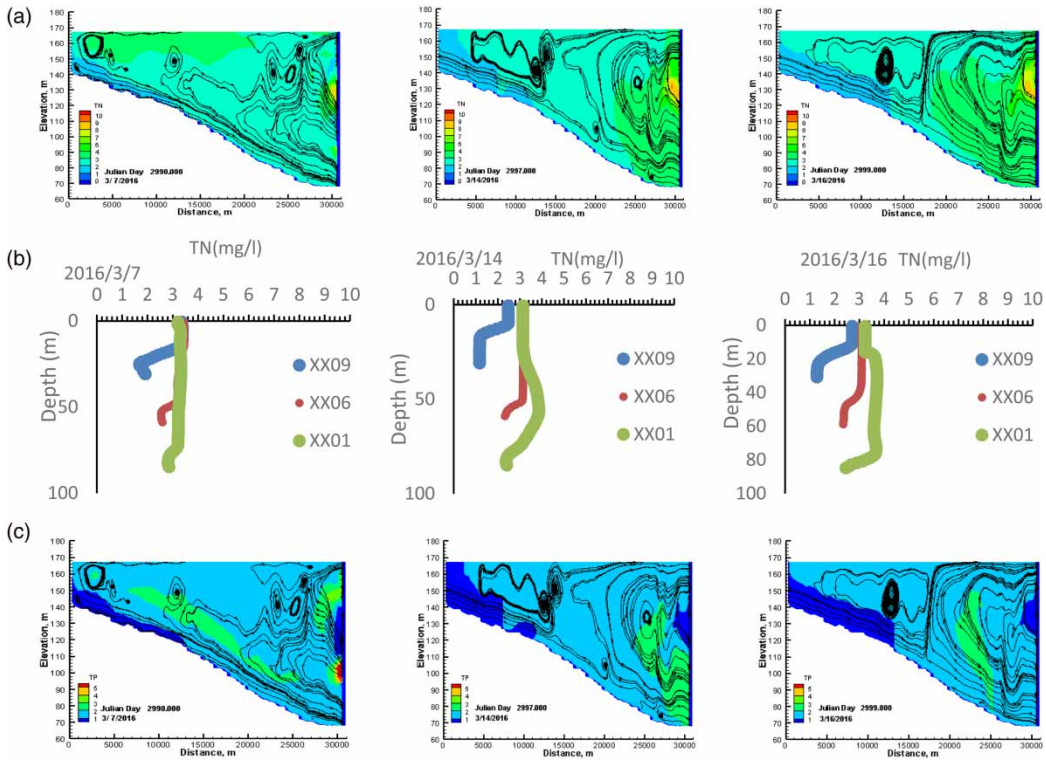


**Figure 11** | (a) Effects of shifts in current patterns on TN longitudinal distribution; (b) Effects of shifts in current patterns on TN longitudinal distribution; (c) Effects of shifts in current patterns on TP concentration.

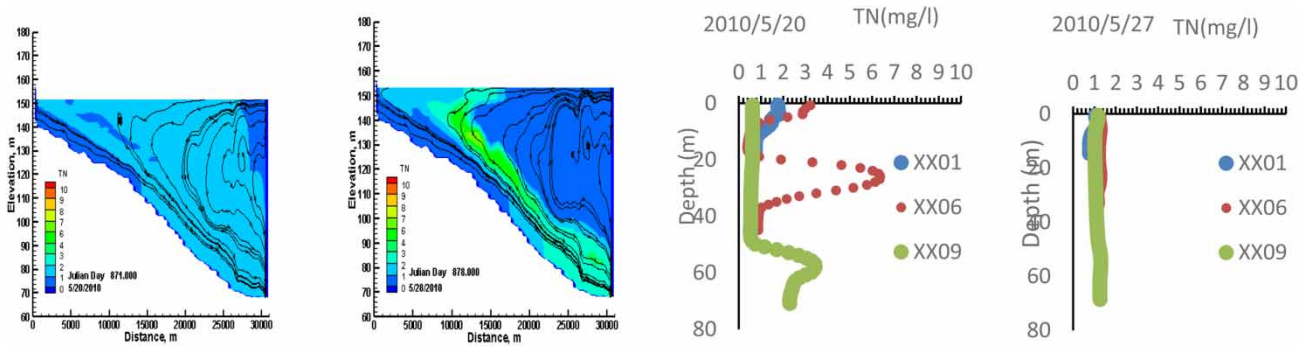


**Figure 12** | Decrease in TN longitudinal distribution on surface due to continuous overflow intrusion.

intensity, are hence are supposed to favor an increase in nutrient distribution on the surface while considering the aforesaid hydrodynamical parameters.

The obvious increase in duration and continuity of overflow intrusion since 2014 during the post cascade reservoirs stage (Ijaz *et al.* 2022) has not substantially increased or decreased average TN distribution on the surface in XXB as shown in Figures 3–14. The trophic status of XXB still remains eutrophic. Increased anthropogenic activities have also not affected average TN, such discrepancies from apparent probabilities could be justified through following simultaneously acting different mechanisms.

Nutrients spatial distribution on the surface also depends on algal blooms because they consume nutrients, so nutrients response to shifts in density currents is not that simple and could not be simply said to be increasing or decreasing. Although overflow intrusions cause strong mixing and more water speed and do not let nutrients to accumulate on surface, water supply

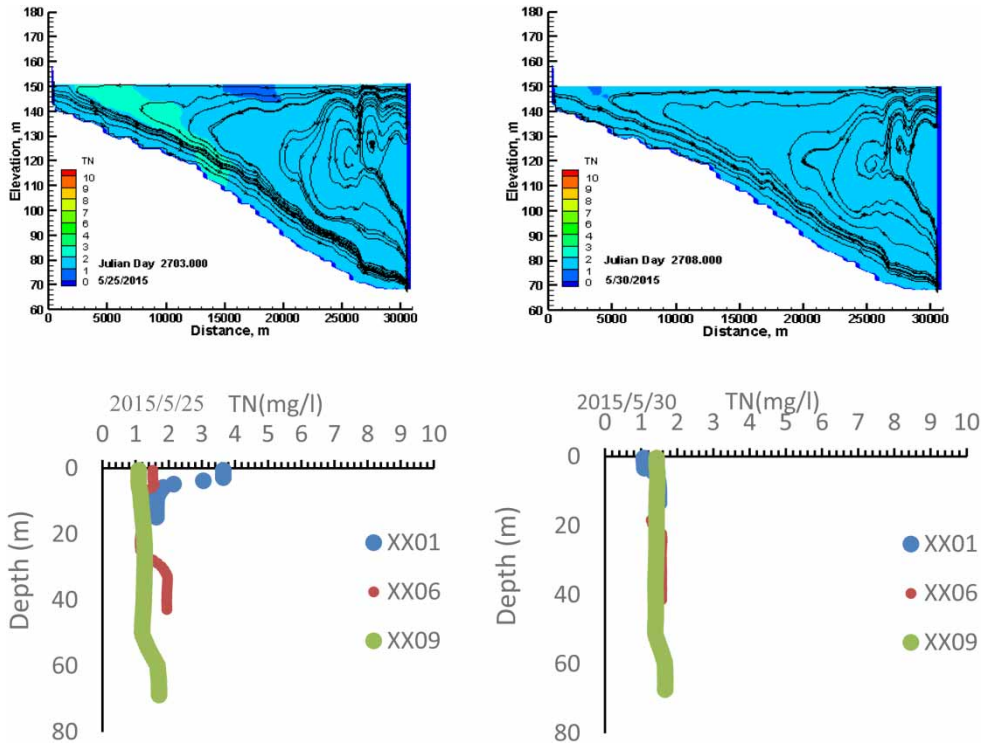


**Figure 13** | Decrease in TN longitudinal distribution on the surface due to continuous overflow intrusion.

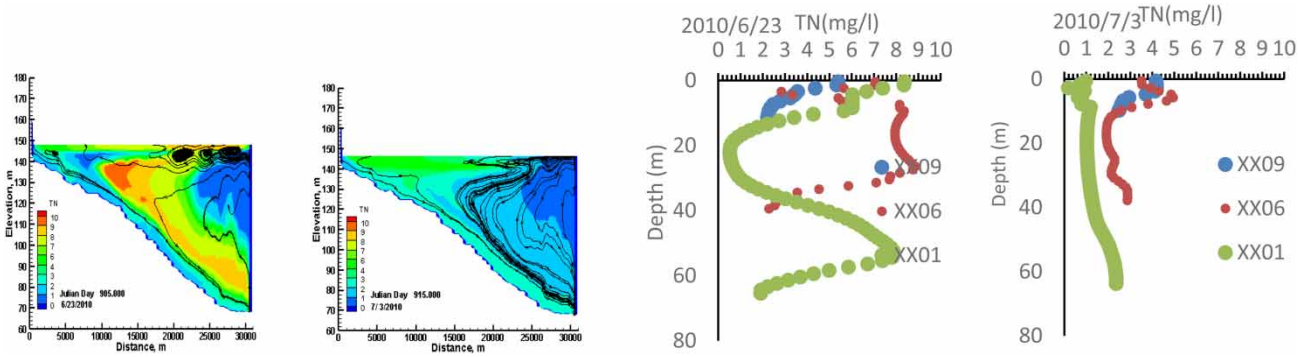


**Figure 14** | Inverse effects of continued current patterns on TN longitudinal distribution

on the surface from the main stream also replenishes nutrients. Similarly, upper interflow and interflow intrusions cause weak mixing, less water speed and cause nutrients to accumulate on the surface, but less intruding water carriage on the surface also supplies less nutrients to the eutrophic zone. Therefore, simultaneous but different ecohydrological affects associated with either of the patterns makes the entire process quite complicated. Nutrients supplied in excess by overflow intrusion and replenishment on the surface could also be facilitated by less mixing following altered upper interflow or interflow to cause eutrophication. Therefore, the volume of intruding water and continuity of circulation patterns for more days become significant through different effects. It is evident from Figures 12 and 13 that overflow intrusion for longer durations could trigger mixing and less accumulation of nutrients at the euphotic zone. As overflow, interflow and upper interflow patterns are prevalent in random order so nutrients could not be predicted theoretically, however nutrients management from non-point sources and the main supplier TGR is advisable. Moreover, the minor average increase in TN corresponds to overflow intrusion points

to maximum supply on surface from the mainstream, whereas less concentrations in March and April by 2010 refer to less supply on the surface from the mainstream due to in depth intrusion. These findings also reflect that eutrophication in XXB could not be studied solely and a modelling approach is required to be extended to all non point sources.

## 5. CONCLUSIONS

Model simulations and plots have contributed notably about alterations in nutrient loading and distributions in XXB with respect to altered density current patterns during pre and post upstream cascade reservoir stages. The following significant conclusions with a wide range of applicability are deduced.

Consequent upon water circulation by overflow intrusion, average TN increased at the upper, middle and lower reaches by 1, 0.5 and 0.1 mg/L respectively overflow intrusion on surface.

The obvious increase in TN on the surface referred to its reliance on the main stream supply, which was maximum following overflow intrusion.

Hydrodynamic parameters such as potential of water exchange and velocity on the surface correspond to reflective density current patterns caused by overflow intrusion and facilitated increased average TN by 1.2 mg/L at the middle and 0.4 mg/L at the upper reaches in spring since 2014. Overflow intrusion was prevalent during pre and post upstream cascade reservoirs stages across all seasons including spring and summer and TN concentration was beyond danger limits triggering eutrophication in XXB.

The highest TN concentration at the upper, middle and lower reaches during April and May was 4, 7.8 and 8.6 mg/L respectively by 2013.

The average TN concentration at the upper, middle and lower reaches during April was 1.9, 3.5 and 4.6 mg/L respectively by 2013. The average TN concentration at the upper, middle and lower reaches during May was 2 mg/L, 3.8 and 5 mg/L respectively by 2013.

Overflow intrusion increased by 30% in spring and 22% in summer during the post-upstream cascade reservoirs stage and have improved TN supply and distribution at the euphotic zone. TN concentration was beyond the danger limit sustaining and prolonging eutrophication status in spring.

The highest TN concentration at the upper, middle and lower reaches during April was 3.7, 7.7 and 9 mg/L respectively since 2014. The highest TN concentration at the upper, middle and lower reaches during May was 3.3, 7.3 and 9.2 mg/L respectively since 2014.

The average TN concentration at the upper, middle and lower reaches during April was 2.1, 3.7 and 4.8 mg/L respectively since 2014. The average TN concentration at the upper, middle and lower reaches during May was 1.9, 3.4 and 4.5 mg/L respectively since 2014.

The decrease at the upper, middle and lower reaches during post dams stage in May was due to the longest continuous prevalence of overflow intrusion and more vertical mixing of nutrients. Despite the reduction in TN longitudinal concentration on surface in May, XXB is still under threat because concentrations were in compliance with pollution indices.

Shifts in density current patterns have complicated impacts on longitudinal TN distribution in spring. It increases following overflow intrusion from the mainstream unless stratification lasts. If overflow intrusion continued for more days, it causes more mixing and TN on the surface started decreasing.

Similarly, upper interflow and interflow intrusion caused a decrease in nutrients supply to the surface, but already accumulated nutrients could rise due to less mixing. The prevalence of upper interflow and interflow intrusion could assist algal growth, which could consume nutrients and reduce their concentration. Therefore nutrients distribution following either of the patterns should be better correlated to temperature stratification and chlorophyll content to find real mechanisms and remedial measures.

Furthermore, detailed research on correlation of density current patterns and their impacts on eutrophication, Chl-a and algal growth in XXB is required for better comprehension of hydro-ecology in XXB. The counter measures to inhibit eutrophication and algal risk are to be tested on the basis of these outcomes.

The variations in distribution of TN concentrations in spring verified the initial increase in TN longitudinal distribution on the surface corresponding to overflow intrusion.

The obvious reduction at the upper, middle and lower reaches corresponding to the longest continuity of overflow intrusion could also be justified through hydrodynamical changes. Upper interflow, interflow and underflow intrusion cause an initial

decrease in TN longitudinal distribution on the surface due to supply cut off from the main stream. These patterns are not likely to increase TN at source but could play their part through hydrodynamical changes in terms of prolonged water age and weak mixing.

TP longitudinal distribution consistently remains less than 0.7 mg/L on average at the upper reach, 0.4 mg/L at the middle reach and 0.23 mg/L at the lower reach despite an exceptional rise in rainy days upstream.

TN/TP ratio across typical years declares XXB as TP limited for eutrophication due to a minor change in TN and TP longitudinal distributions.

Eutrophication and algal growth in XXB remained TP limited over the entire period with few exceptions at the upper reach. Although TP increased at the lower reach, eutrophication remained TP limited for most of the cases with few exceptions.

Average TN increased by 0.1, 0.3 and 0.5 mg/L at the upper, middle and lower reaches respectively in late March since 2014 compared to those in the early years. It increased by 0.2, 0.4 and 0.6 mg/L at the upper, middle and lower reaches in early April since 2014. It increased by 0.3, 0.6, and 0.9 mg/L at the upper, middle and lower reaches in mid April since 2014. It increased a bit at the upper reach, 0.6 mg/L at the middle reach and 0.9 mg/L at the lower reach during late April. It increased a bit at the upper reach, by 0.3 mg/L at the middle reach and by 0.5 mg/L at the lower reaches corresponding to either of the patterns. During mid May, it remained the same at the upper reach, and decreased by 0.2 mg/L at the middle reach and 0.5 mg/L at the lower reaches. During late May, it remained the same at the upper reach, decreased by 0.4 mg/L at the middle reach and 0.6 mg/L at the lower reaches. These statistics indicate average increase in TN in spring except in late May.

Distribution of all water quality parameters such as TP, nitrite/nitrate ($NO^2/NO^3$), ammonia/ammonium ($NH^3/NH^4$) and TN is required to be evaluated further with respect to internal and external resources.

A particle trace method should also be adopted for the entire period to elucidate nutrients transportation and shifting trends across seasons. Model yielded values could help to devise strategies of reducing watershed nutrient loads. Findings point to the dire need for sagacious nutrient management into XXB to mitigate algal bloom in the tributary bay. This management policy should be extended to the main stream, which is the main supplier of nutrients and other non-point sources.

The total nitrogen of XXB showed a high level. The nitrogen concentration of the upstream was increased since 2014, but remained lower than that at the downstream. Although phosphorus concentration at the downstream was increased since 2014, it still remained lower than that at the upstream. The nitrogen and phosphorus concentrations were higher than the threshold of eutrophication.

The mechanisms behind spatiotemporal variations in TN and TP and limitation factor could not be investigated without correlation with algal blooms and chlorophyll-a, because algal blooms consume total dissolved nitrogen and phytoplankton often build up their intracellular nutrient pools via luxury consumption.

## DATA AVAILABILITY STATEMENT

All relevant data are included in the paper or its Supplementary Information.

## CONFLICT OF INTEREST

The authors declare there is no conflict.

## REFERENCES

Ai, Y., Bi, Y. & Hu, Z. 2015 Changes in phytoplankton communities along nutrient gradients in Lake Taihu: evidence for nutrient reduction strategies. *JOL* **33**, 447–457.

Ambrose, R. B., Wool, T. A. & Barnwell, T. O. 2009 Development of water quality modeling in the United States. *Environmental Engineering Research* **14**, 200–210.

Andersen, I. M., Williamson, T. J., González, M. J. & Vanni, M. J. 2020 Nitrate, ammonium, and phosphorus drive seasonal nutrient limitation of chlorophytes, cyanobacteria, and diatoms in a hyper-eutrophic reservoir. *Limnology and Oceanography* **65**, 962–978.

Atique, U. & An, K.-G. 2019 Reservoir water quality assessment based on chemical parameters and the chlorophyll dynamics in relation to nutrient regime. *Polish Journal of Environmental Studies* **28**, 322–329.

Bartosiewicz, M., Laurion, I., Clayer, F. & Maranger, R. 2016 Heat-wave effects on oxygen, nutrients, and phytoplankton can alter global warming potential of gases emitted from a small shallow lake. *Environmental Science & Technology* **50**, 6267–6275.

Bartosiewicz, M., Przytulska, A., Deshpande, B. N., Antoniades, D., Cortes, A., MacIntyre, S., Lehmann, M. F. & Laurion, I. 2019 Effects of climate change and episodic heat events on cyanobacteria in a eutrophic polymictic lake. *Science of the Total Environment* **693**, 133414.

Bernhardt, E. S. 2013 Cleaner lakes are dirtier lakes. *Science* **342**, 205–206.

Bowen, J. D. & Hieronymus, J. W. 2003 A CE-QUAL-W2 model of Neuse Estuary for total maximum daily load development. *Journal of Water Resources Planning and Management* **129**, 283–294.

Chen, S., Little, J. C., Carey, C. C., McClure, R. P., Lofton, M. E. & Lei, C. 2018 Three-dimensional effects of artificial mixing in a shallow drinking-water reservoir. *Water Resources Research* **54**, 425–441.

Chuo, M., Ma, J., Liu, D. & Yang, Z. 2019 Effects of the impounding process during the flood season on algal blooms in Xiangxi Bay in the Three Gorges Reservoir, China. *Ecological Modelling* **392**, 236–249.

Cole, T. & Wells, S. 2013 *CE-QUAL-W2: A two-Dimensional, Laterally Averaged, Hydrodynamic and Water Quality Model, Version 3.71*. User Manual, Department of Civil and Environmental Engineering, Portland State University, Portland.

Coronado-Franco, K. V., Selvaraj, J. J. & Pineda, J. E. M. 2018 Algal blooms detection in Colombian Caribbean Sea using MODIS imagery. *Marine Pollution Bulletin* **133**, 791–798.

Costa, C. M. d. S. B., da Silva Marques, L., Almeida, A. K., Leite, I. R. & de Almeida, I. K. 2019 Applicability of water quality models around the world – a review. *Environmental Science and Pollution Research* **26**, 36141–36162.

El-Serehy, H. A., Abdallah, H. S., Al-Misned, F. A., Al-Farraj, S. A. & Al-Rasheid, K. A. 2018 Assessing water quality and classifying trophic status for scientifically based managing the water resources of the Lake Timsah, the lake with salinity stratification along the Suez Canal. *Saudi Journal of Biological Sciences* **25**, 1247–1256.

Finlay, J. C., Small, G. E. & Sterner, R. W. 2013 Human influences on nitrogen removal in lakes. *Science* **342**, 247–250.

Gao, Q., He, G., Fang, H., Bai, S. & Huang, L. 2018 Numerical simulation of water age and its potential effects on the water quality in Xiangxi Bay of Three Gorges Reservoir. *Journal of Hydrology* **566**, 484–499.

Huang, Y., Li, Y., Ji, D., Nwankwegu, A. S., Lai, Q., Yang, Z., Wang, K., Wei, J. & Norgbey, E. 2020 Study on nutrient limitation of phytoplankton growth in Xiangxi Bay of the Three Gorges Reservoir, China. *Science of the Total Environment* **723**, 138062.

Ijaz, U., Cheng, Z. & Qiu, S. 2022 Evolutionary mechanisms and shifting trends in water circulation patterns in a tributary of the Three Gorges Reservoir, China. *Water Supply* **38**, 169–178.

Ji, D., Wells, S. A., Yang, Z., Liu, D., Huang, Y., Ma, J. & Berger, C. J. 2017 Impacts of water level rise on algal bloom prevention in the tributary of Three Gorges Reservoir, China. *Ecological Engineering* **98**, 70–81.

Jin, J., Wells, S. A., Liu, D., Yang, G., Zhu, S., Ma, J. & Yang, Z. 2019 Effects of water level fluctuation on thermal stratification in a typical tributary bay of Three Gorges Reservoir, China. *PeerJ* **7**, e6925.

Kim, H. G., Hong, S., Jeong, K.-S., Kim, D.-K. & Joo, G.-J. 2019 Determination of sensitive variables regardless of hydrological alteration in artificial neural network model of chlorophyll a: case study of Nakdong River. *Ecological Modelling* **398**, 67–76.

Lai, X., Liang, Q., Jiang, J. & Huang, Q. 2014 Impoundment effects of the Three-Gorges-Dam on flow regimes in two China's largest freshwater lakes. *Water Resources Management* **28**, 5111–5124.

Li, Z., Ma, J., Guo, J., Paerl, H. W., Brookes, J. D., Xiao, Y., Fang, F., Ouyang, W. & Lunhui, L. 2019 Water quality trends in the Three Gorges Reservoir region before and after impoundment (1992–2016). *Ecohydrology & Hydrobiology* **19**, 317–327.

Li, X., Liu, B., Wang, Y., Yang, Y., Liang, R., Peng, F., Xue, S., Zhu, Z. & Li, K. 2020a Hydrodynamic and environmental characteristics of a tributary bay influenced by backwater jacking and intrusions from a main reservoir. *Hydrology and Earth System Sciences* **24**, 5057–5076.

Li, Y., Sun, J., Lin, B. & Liu, Z. 2020b Thermal-hydrodynamic circulations and water fluxes in a tributary bay of the Three Gorges Reservoir. *Journal of Hydrology* **585**, 124319.

Liu, L., Liu, D., Johnson, D. M., Yi, Z. & Huang, Y. 2012 Effects of vertical mixing on phytoplankton blooms in Xiangxi Bay of Three Gorges Reservoir: implications for management. *Water Research* **46**, 2121–2130.

Long, L., Ji, D., Yang, Z., Ma, J., Wells, S. A., Liu, D. & Lorke, A. 2019 Density-driven water circulation in a typical tributary of the Three Gorges Reservoir, China. *River Research and Applications* **35**, 833–843.

Ly, J., Philippart, C. J. & Kromkamp, J. C. 2014 Phosphorus limitation during a phytoplankton spring bloom in the western Dutch Wadden Sea. *Journal of Sea Research* **88**, 109–120.

Ma, J., Liu, D., Wells, S. A., Tang, H., Ji, D. & Yang, Z. 2015 Modeling density currents in a typical tributary of the Three Gorges Reservoir, China. *Ecological Modelling* **296**, 113–125.

Mamun, M. & An, K.-G. 2017 Major nutrients and chlorophyll dynamics in Korean agricultural reservoirs along with an analysis of trophic state index deviation. *Journal of Asia-Pacific Biodiversity* **10**, 183–191.

Nwankwegu, A. S., Li, Y., Huang, Y., Wei, J., Norgbey, E., Lai, Q., Sarpong, L., Wang, K., Ji, D. & Yang, Z. 2020 Nutrient addition bioassay and phytoplankton community structure monitored during autumn in Xiangxi bay of three gorges reservoir, China. *Chemosphere* **247**, 125960.

Nwankwegu, A. S., Li, Y., Zhang, L., Huang, Y., Xie, D., Norgbey, E. & Paerl, H. W. 2021 *Spatial Biomass Production and Seasonal Nutrient Limitation Transitions in A Tributary of The Three Gorges Reservoir, China*.

Paerl, H. W., Scott, J. T., McCarthy, M. J., Newell, S. E., Gardner, W. S., Havens, K. E., Hoffman, D. K., Wilhelm, S. W. & Wurtsbaugh, W. A. 2016 It takes two to tango: when and where dual nutrient (N & P) reductions are needed to protect lakes and downstream ecosystems. *Environmental Science & Technology* **50**, 10805–10813.

Passy, P., Le Gendre, R., Garnier, J., Cugier, P., Callens, J., Paris, F., Billen, G., Riou, P. & Romero, E. 2016 Eutrophication modelling chain for improved management strategies to prevent algal blooms in the Bay of Seine. *Marine Ecology Progress Series* **543**, 107–125.

Saadatpour, M., Afshar, A. & Edinger, J. E. 2017 Meta-model assisted 2D hydrodynamic and thermal simulation model (CE-QUAL-W2) in deriving optimal reservoir operational strategy in selective withdrawal scheme. *Water Resources Management* **31**, 2729–2744.

Sepehri, A., Sarrafzadeh, M.-H. & Avateffazeli, M. 2020 Interaction between Chlorella vulgaris and nitrifying-enriched activated sludge in the treatment of wastewater with low C/N ratio. *Journal of Cleaner Production* **247**, 119164.

Shabani, A., Zhang, X. & Ell, M. 2017 Modeling water quantity and sulfate concentrations in the Devils Lake watershed using coupled SWAT and CE-QUAL-W2. *JAWRA Journal of the American Water Resources Association* **53**, 748–760.

Smith, V. H. 1982 The nitrogen and phosphorus dependence of algal biomass in lakes: An empirical and theoretical analysis 1. *Limnology and Oceanography* **27**, 1101–1111.

Smith, E. A., Kiesling, R. L., Galloway, J. M. & Ziegeweid, J. R. 2014 *Water quality and algal community dynamics of three deepwater lakes in Minnesota utilizing CE-QUAL-W2 models*. US Geological Survey.

Spears, B. M., Carvalho, L., Dudley, B. & May, L. 2013 Variation in chlorophyll a to total phosphorus ratio across 94 UK and Irish lakes: implications for lake management. *Journal of Environmental Management* **115**, 287–294.

Stow, C. A., Cha, Y., Johnson, L. T., Confesor, R. & Richards, R. P. 2015 Long-term and seasonal trend decomposition of Maumee River nutrient inputs to western Lake Erie. *Environmental Science & Technology* **49**, 3392–3400.

Sun, J., Lin, J., Zhang, X., Xiao, Z., Lin, B. & Xu, H. 2021 Dam-influenced seasonally varying water temperature in the Three Gorges Reservoir. *River Research and Applications* **37**, 579–590.

Wang, Y., Zhang, N., Wang, D., Wu, J. & Zhang, X. 2018 Investigating the impacts of cascade hydropower development on the natural flow regime in the Yangtze River, China. *Science of the Total Environment* **624**, 1187–1194.

Wu, D., Yan, H., Shang, M., Shan, K. & Wang, G. 2017 Water eutrophication evaluation based on semi-supervised classification: a case study in Three Gorges Reservoir. *Ecological Indicators* **81**, 362–372.

Xia, J., Xu, G., Guo, P., Peng, H., Zhang, X., Wang, Y. & Zhang, W. 2018 Tempo-spatial analysis of water quality in the Three Gorges Reservoir, China, after its 175-m experimental impoundment. *Water Resources Management* **32**, 2937–2954.

Xiang, R., Wang, L., Li, H., Tian, Z. & Zheng, B. 2021 Temporal and spatial variation in water quality in the Three Gorges Reservoir from 1998 to 2018. *Science of The Total Environment* **768**, 144866.

Xu, H., Yan, M., Long, L., Ma, J., Ji, D., Liu, D. & Yang, Z. 2021 Modeling the effects of hydrodynamics on thermal stratification and algal blooms in the Xiangxi Bay of Three Gorges Reservoir. *Frontiers in Ecology and Evolution* **453**, 188–197.

Yang, Z., Yu, Y., Chen, Z. & Ma, J. 2017 Mechanism of eutrophication and phytoplankton blooms in Three Gorges Reservoir, China: a research review. *Engineering Journal of Wuhan University* **50**, 507–516.

Yang, Z., Cheng, B., Xu, Y., Liu, D., Ma, J. & Ji, D. 2018a Stable isotopes in water indicate sources of nutrients that drive algal blooms in the tributary bay of a subtropical reservoir. *Science of the Total Environment* **634**, 205–213.

Yang, Z., Xu, P., Liu, D., Ma, J., Ji, D. & Cui, Y. 2018b Hydrodynamic mechanisms underlying periodic algal blooms in the tributary bay of a subtropical reservoir. *Ecological Engineering* **120**, 6–13.

Yu, Z. & Wang, L. 2011 Factors influencing thermal structure in a tributary bay of Three Gorges Reservoir. *Journal of Hydrodynamics. Ser. B* **23**, 407–415.

Yuan, L. L., Pollard, A. I., Pather, S., Oliver, J. L. & D'Anglada, L. 2014 Managing microcystin: identifying national-scale thresholds for total nitrogen and chlorophyll a. *Freshwater Biology* **59**, 1970–1981.

Zhao, Y., Wang, Y. & Wang, Y. 2021 Comprehensive evaluation and influencing factors of urban agglomeration water resources carrying capacity. *Journal of Cleaner Production* **288**, 125097.

Zhou, Z.-X., Yu, R.-C. & Zhou, M.-J. 2017 Resolving the complex relationship between harmful algal blooms and environmental factors in the coastal waters adjacent to the Changjiang River estuary. *Harmful Algae* **62**, 60–72.

First received 8 May 2022; accepted in revised form 17 July 2022. Available online 18 August 2022